Journal of Hydrology 567 (2018) 590–604

Contents lists available at ScienceDirect

Journal of Hydrology

journal homepage: www.elsevier.com/locate/jhydrol

Research papers

Identifying the dominant controls on macropore flow velocity in soils: A meta-analysis

Man Gao[a,1], Hong-Yi Li[b,*,1], Dengfeng Liu[c,1], Jinyun Tang[d], Xingyuan Chen[e], Xi Chen[a,f], Günter Blöschl[g], L. Ruby Leung[e]

[a] Institute of Surface-Earth System Science, Tianjin University, Tianjin, China
[b] Department of Civil and Environmental Engineering, University of Houston, Houston, Texas, USA
[c] State Key Laboratory Base of Eco-hydraulic Engineering in Arid Area, School of Water Resources and Hydropower, Xi'an University of Technology, Xi'an, China
[d] Lawrence Berkeley National Laboratory, Berkeley, CA, USA
[e] Pacific Northwest National Laboratory, Richland, WA, USA
[f] State Key Laboratory of Hydrology-Water Resources and Hydraulic Engineering, College of Hydrology and Water Resources, Hohai University, Nanjing, China
[g] Institute of Hydraulic Engineering and Water Resources Management, Vienna University of Technology, Vienna, Austria

ARTICLE INFO

This manuscript was handled by Marco Borga, Editor-in-Chief, with the assistance of Christian Massari, Associate Editor

Keywords:
Macropore flow velocity
Meta-analysis
Observation scale
Macropore diameter
Rainfall intensity
Macropore network connectivity

ABSTRACT

Macropore flow is a ubiquitous hydrologic process that has not been well explained using traditional hydrologic theories. In particular, macropore flow velocity (MFV) is poorly understood with respect to its typical ranges and controlling factors. Here we conducted a meta-analysis based on an MFV dataset compiled from 243 measurements documented in 76 journal articles. The dataset includes MFV values measured using different approaches across the soil-core, field-profile, and trench scales. Our analyses show that MFV has a geometric mean of 1.08×10^{-3} m s^{-1}, which is about 2~3 orders of magnitude larger than the corresponding values of saturated hydraulic conductivity in the soil matrix. Using machine learning methods including classification and regression tree and random forests algorithms, we identified observation scale, travel distance, rainfall intensity and macropore diameter as the most important factors that control MFV. MFV is much larger at the trench scale than at the other two scales mainly due to abundant large macropores. Correlation analysis and multivariate regression revealed that (1) MFV and rainfall intensity have significant positive correlation, which indicates that MFV is a dynamic variable; and (2) MFV and macropore diameter also have strong positive correlation at the trench scale, which indicates macropore size as a key controlling factor. Using macropore diameter and rainfall intensity as explanatory factors, MFV can be well predicted ($R^2 = 0.76$) by a multivariate regression equation at trench-scale, implying that rainfall intensity can be considered a proxy for the filling degree of macropores. Furthermore, both the Poiseuille and Manning equations were found to overestimate the MFV values, suggesting a parameter representing the connectivity of the macropore network is needed for providing reasonable estimates of MFV using physically-based equations.

1. Introduction

Macropores are large soil voids with features that are distinct from the soil matrix (Cey and Rudolph, 2009). They are ubiquitous in soils and function as fast channels, bypassing the soil matrix and expediting the movement of water and solutes below ground both vertically and horizontally. Macropore flow (MF) has been identified as a significant contributor to streamflow across diverse climate regions, from semi-arid to humid and from tropical to cold regions (Koch et al., 2013; dos Santos et al., 2016; Van Schaik et al., 2008; Zhu, 1997; Negishi et al., 2007; Uchida et al., 2005; Jones, 2010). MF also has great influences on infiltration, soil moisture distribution (Hardie et al., 2011; Hardie et al., 2013) and groundwater table dynamics (Mirus and Nimmo, 2013). Hence effectively representing MF in hydrologic models is important for improving soil moisture and streamflow prediction and water management (Zehe et al., 2007; 2010; Beven and Germann, 2013; Weiler, 2017; Alaoui et al., 2018).

The most important variable to represent MF is the average velocity of water traveling through the macropores, denoted as macropore flow velocity (MFV), which is the rate of the macropore flux in macropores.

* Corresponding author.
E-mail address: hli57@uh.edu (H.-Y. Li).
[1] Formerly at Department of Land Resources and Environmental Sciences, Montana State University, Bozeman, MT, USA

https://doi.org/10.1016/j.jhydrol.2018.10.044
Received 7 May 2018; Received in revised form 6 July 2018; Accepted 18 October 2018
Available online 23 October 2018

MFV determines the strength and significance of MF in simulations of subsurface flow and solute transport (Jarvis, 2007; Anderson et al., 2009b). It is usually much larger than the travel velocity of water through soil matrix, which is mostly estimated using saturated hydraulic conductivity (K_s) and hydraulic head gradient. MFV is primarily a function of water storage in the macropores and the structure of macropores (density of macropores in the soil, diameter of macropores, macropore networks etc.). However, the structure of macropore co-evolves with the soil structure (e.g., cracks and fissures), soil fauna and plant roots, and other surface and subsurface properties (Beven and Germann, 1982) so measuring or precisely describing the structure of macropores has been challenging.

The MFV values have also been directly set in several studies instead of deriving them with macropore structure or other information. The simplest way to estimate MFV is to relate it to K_s by a ratio. For example, Yu et al. (2014) suggested using MFV that is 100 times the value of K_s to represent the MF process. Since MFV is always much larger than K_s, Dusek et al. (2012) assumed MFV at a fixed value of 5000 cm d^{-1} for measured K_s ranging from 1.3 to 567 cm d^{-1} at different soil horizons. The Poiseuille equation and Manning equation have also been adopted (Chen and Wagenet, 1992; Köhne et al., 2009) to provide a reference value of MFV.

Although the aforementioned approaches have been shown to provide reasonable estimates of MFV, there is no general guidance on appropriate values to be used across basins of different characteristics. Hence estimating MFV through experiments is often preferred. Artificial tracer is the most popular approach applied to empirically quantify MFV. At soil-core scale, Luo et al. (2008) measured MFV by applying tracer and computed the velocity as a function of travel time and vertical distance. At field-profile scale, Cey and Rudolph (2009) used dye tracer to track the occurrence of film and rivulet flow along vertical macropores and obtained flow velocity. Soil-core scale measurements often ignore the effect of large-scale heterogeneities because the structure and the connectivity of macropore network cannot be represented at such a scale. Experiments at the hillslope scale, on the other hand, can better represent the large-scale heterogeneity and produce more reasonable MFV estimates. Anderson et al. (2009a and 2009b) quantified hillslope-scale MFV by excavating a trench and applying steady artificial rainfall with NaCl added at the upper hillslope as a tracer. Cheng et al. (2009) estimated MFV by using hydrographs from individual macropores at an excavated trench profile. However, such experiments are time-consuming and labor-intensive. A feasible alternative is to establish relationships between MFV and its controlling factors (e.g., soil properties, land use, water supply conditions) to enable estimation of MFV a priori from existing information.

Several studies have been conducted to explore the main controlling factors of MFV. Anderson et al. (2009b) found that MFV is most closely related to the 1-h rainfall intensity and slope length. Mosley (1982) indicated that MFV varies as a function of antecedent moisture conditions and the relative importance of various pathways at a given site, which are in turn functions of macropore network and soil properties. Uchida et al. (2001) concluded that MFV depends on macropore diameter and its value is generally larger in peaty soil than in forest soil. These studies have been conducted at single or multiple hillslopes; there are also studies that considered a wider range of sites and controls. For example, Jarvis et al. (2009) suggested that soil susceptibility to MF could be predicted from easily available soil properties and site factors. Koestel et al. (2012) collected 733 breakthrough curves from the literature and found that moderate-to-strong MF occurs only for undisturbed soils that contain more than 8% clay. Similarly, Koestel and Jorda (2014) demonstrated that soil susceptibility to MF under steady state conditions is predictable from proxy variables to a large extent, such as the clay content, ratio between clay content and organic carbon, and lateral observation scale. Jarvis et al. (2013) defined the largest macropore hydraulic conductivity ($K_{s(ma)}$) for large soil pores (diameter $>$ 0.3 mm) and found that its value is related to soil texture and soil bulk density. Although the magnitudes of both MF and $K_{s(ma)}$ are related to MFV, they cannot reflect the true flow velocity along the macropore network. Despite these studies, there is no consensus on the most appropriate physical or empirical equations to be used for the estimate MFV values, and comprehensive studies on the identification of the general controls on MFV across diverse hillslopes and scales are still in need. Weiler (2017) called for community efforts to combine existing datasets to allow inter-comparison studies as it has been successfully performed in many other scientific fields. A meta-analysis approach (e.g., Mutema et al., 2015) may be an effective way to address this need.

This study presents a meta-analysis conducted to compile a dataset from the published literature that reported measured MFVs from empirical experiments and a series of relevant controlling factors. The dataset was then analyzed with multiple methods. Machine learning algorithms including classification and regression tree and random forests were employed to identify the main controlling factors of MFV. Correlation analysis and multivariate regression were used to determine empirical relationships between MFV and its main controlling factors. Our objective is three-fold: (1) to establish general ranges and typical values of MFV at different scales, (2) to identify the dominant factors controlling MFV, and (3) to provide guidance for estimating MFV in the field, especially at hillslope scale.

2. Data and methods

2.1. Compiling the dataset

In this study, MFV is defined as the velocity of water traveling through macropores. Measurements of MFV values were collected from the published literature through Google Scholar search. The criteria for including a publication are: (1) the MFV values are obtained from experiments, (2) the experiments are conducted in undisturbed soils, (3) the occurrence of macropore flow is obvious, (4) sufficient information about the experiments and sites is provided, (5) the MFV values are either directly presented in the work or can be indirectly estimated by using the provided information, and (6) the approaches used to estimate MFV belongs to a screened group in order to ensure a common ground where a comparison among MFV values differently derived can be made. On the basis of these criteria, a dataset consisting of 243 individual data points compiled from 76 published studies was realized. Among the various experimental approaches for MF, only five explicitly provide the MFV values, which are briefly described below.

2.1.1. Artificial tracer

Artificial tracer is the most common and effective approach to determine MFV at different scales. The velocity of macropore flow (V) can be obtained by fitting the measured breakthrough curves using the convection-dispersion equation or by dividing the travel distance by travel time. There are two kinds of travel time (T) usually used to calculate MFV, i.e., peak travel time and first arrival travel time. According to the analytical solution of the convection-dispersion equation for solute transport (Jury et al., 1991), the peak travel time is more suitable for calculating the mean MFV and is preferred in our analysis. If the peak travel time is absent, MFV derived from the first arrival travel time is selected. Most MFV values adopted here are obtained using peak travel time and breakthrough curve fitting.

2.1.2. Non-sequential soil moisture response

Generally, during a rainfall period a wetting front moves gradually from the top to the bottom in a homogeneous soil profile. The soil moisture content in the upper part of the soil responds faster than that in the lower part. Thus, the soil moisture content increases sequentially from the upper part to the lower part. With macropore flow, the sequential response of soil moisture content with depth can be violated. Lin and Zhou (2008) defined preferential flow operationally as an

increase in soil water content out of sequence with respect to soil depth. With this consideration, we collected velocity values calculated under the no-sequence soil water moisture response condition. In this approach, MFV values are also calculated by dividing the travel distance by the response time.

2.1.3. Hydraulic conductivity and macroporosity

Macropores are usually identified as pores of equivalent cylindrical diameter larger than 0.3 ~ 1 mm (Luxmoore, 1981; Jarvis, 2007), which is corresponding to capillary potential (φ) of 3~10 hPa. Flow velocity in macropores can be estimated by combining the information of macroporosity (ε) and amount of water flowing through them. Once the flow flux (q_s) under saturated condition and near saturation hydraulic conductivity ($K(\varphi)$) with capillary potential (φ = 3~10 hPa) are obtained, the contribution of macropore to q_s can be calculated as $q_s - K(\varphi)$. Considering the portion of water moving through macropores, the mean velocity of flow through the macropore can be given as

$$V = [q_s - K(\varphi)]/\varepsilon \quad (1)$$

ε can be estimated by the difference between water content at $\varphi = 0$ and φ = 3~10 hPa or directly measured by X-ray Computed Tomography.

2.1.4. Individual macropore discharge

Macropore flow rate can be directly measured at an excavated trench or road-cut cross-section. The corresponding MFV can be estimated by dividing the macropore discharge (Q_{mac}) by macropore cross-sectional area (A_{mac}). A series of observed Q_{mac} can be obtained under different conditions. We used the largest value of Q_{mac} when calculating MFV.

2.1.5. Rainfall-Runoff lag

When macropore flow is the dominant component in discharge in a storm event, the lag time between hyetograph and hydrograph centroid represents the mean transport time of macropore flow under wet condition (Mosley, 1982). At small scales, the mean MFV value during a storm event can be estimated by dividing the mean travel distance by the centroid lag time of hyetograph and hydrograph.

Table 1 lists the number of publications and data points corresponding to each approach described above. Furthermore, all the field and laboratory experimental data are also classified according to the experiment scales, i.e., trench (hillslope) scale, field-profile scale and soil-core (soil-column) scale. The trench scale experiments were conducted at hillslopes with travel distances ranging from several meters to 100 m (17.8 m on average). At field-profile scale, the vertical infiltration process dominates, and the travel distance is around 0.82 m. At the soil-core scale, the experiments were undertaken either in the field or the laboratory with travel distances less than 0.5 m (0.18 m on average). All publications used to compile the dataset are listed in the appendix.

2.2. Methods of identifying controlling factors

We begin with ten local factors that are considered to potentially control MFV, including boundary condition factors, experimental factors, and physical factors of the experiment sites. The boundary condition factor is mainly represented by the artificial or natural rainfall intensity during the experiments (here no distinction is made between the two kinds of rainfall conditions). Experimental factors include the observation scales (i.e., soil-core, field-profile, or trench), travel distance and experimental conditions (artificial rainfall, natural rainfall, injection, or ponding). Regarding the experimental conditions, injection means water is injected to a specific depth below the soil surface by trench or drilled hole, and ponding means that the experiments are conducted with water pressure greater than zero at the soil surface. Physical factors include soil types (clayey, loamy, sandy, and silty soil), land use (forest, grassland, and farmland), macropore diameter, mean annual precipitation, K_s, and slope gradient. Soil types were reclassified following Jarvis et al. (2009): (1) clay, sandy clay, silty clay, sandy clay loam, clay loam, and silty clay loam were grouped as clayey soil, (2) sand, loamy sand, and sandy loam were grouped as sandy soil, (3) silt and silty loam were grouped as silty soil, and 4) loam was separately listed as loamy soil. More detailed descriptions of each factor are provided in Table 2.

2.3. Methods of analysis

Three steps were used to analyze the relationships between MFV and its controlling factors. In the first step, two machine learning methods, classification and regression tree and random forests, were used to identify the most dominant controlling factors of MFV. In the second step, correlation analysis and multivariate linear regression methods were used to reveal the correlations of the identified controlling factors and MFV. Lastly, empirical equations were derived to estimate MFV as a function of the identified controlling factors. These steps are described in more detail below.

2.3.1. Classification and regression tree

Classification and regression tree (CART) is a non-parametric technique for sequential partitioning of a dataset composed of a response variable and any number of potential predictor variables using dichotomous criteria (Breiman et al., 1984). Following Breiman (2001), three steps were undertaken to build a regression tree. First, recursive binary splitting was used to grow a large tree on the training data until each terminal node has fewer than a given minimum number of observations. Then, a complexity parameter was used to prune the large tree in order to obtain the sequence of the best subtrees. Finally, *k*-fold cross-validation was used to test the accuracy of the generated regression tree and optimize the nodes or splitters of the tree. At each split, the technique searches for the predictor variable that provides the most effective binary separation of the range in the response variable (Rothwell et al., 2008). In each group, values of the response variable have to be as homogeneous as possible, aiming at minimizing the

Table 1
Statistics of the dataset established by data points and publication numbers from literature.

Measurement approach	Soil-core scale		Field-profile scale		Trench scale		Total	
	Data points	Publications	Data points	Publications	Data points	Publications	Data points	Publications
Artificial tracer	24	5	28	15	92	26	144	46
No-sequence soil moisture response	10	1	10	4	0	0	20	5
Hydraulic conductivity and macroporosity	60	19	0	0	0	0	60	19
Macropore discharge	0	0	0	0	13	4	14	4
Rainfall-Runoff lag	0	0	1	1	5	2	6	3
Total	94	25	39	20	110	32	243	76*

* Comment: there is one publication containing both scale soil-core and trench scale data points.

Table 2
Overview of the considered predictors of MFV.

Predictor type	Abbreviation	Unit	Numbers	Description
Observation scale	*Scale*	–	243	Soil-core; Field-profile; Trench
Experimental condition	*Condition*	–	243	Artificial rainfall; Nature rainfall; injection; Ponding
Soil type	*Soil*	–	204	Sandy (Sd); Silty (St); Loamy (Lm); Clayey (Cl)
Land use	*Land*	–	242	Forest; Grassland; Farmland
Travel distance	*L*	cm	243	
Macropore diameter	*D*	mm	74	
Rainfall intensity	*I*	$mm\ h^{-1}$	95	
Mean annual precipitation	*P*	$mm\ a^{-1}$	140	
Saturated hydraulic conductivity	*Ks*	$m\ s^{-1}$	221	
Slope gradient	*S*	–	110	Only available at trench scale

overall deviance.

The importance of the variables selected in CART was assessed by the total reduction in the residual sum of squares (RSS) achieved by all splitting nodes on that predictor variable after the regression tree is generated (Prasad et al., 2006). They were also scaled to sum to 100% and any variable with contribution less than 1% was considered insignificant.

2.3.2. Random forests

Random forests (RF) is an ensemble of un-pruned regression trees that are grown on bootstrap samples (Koestel and Jorda, 2014). When a bootstrap resample is drawn, 1/3 of the data were excluded from the sample, while the remaining data were replicated to bring the sample back to the full size. The portion of the data drawn into the sample in a replication is known as the "in-bag" data (2/3 of the data), whereas the portion not drawn is the "out-of-bag" data (1/3 of the data). The latter were not used to build or prune any tree but provide better estimates of node error and other generalization errors for bagged predictors. When building each tree, the number of predictors (n_p) used to find the best split at each node was a randomly chosen subset of the total number of predictors (m). $n_p \approx \sqrt{m}$ was used as recommended by James et al. (2013).

We used two measures of variable importance. The first one is the increase in mean squared error (MSE) if one predictor variable is removed, which is the increase of prediction accuracy for the out-of-bag data as a result of the predictor variable being permuted. The MSEs were then averaged over all the trees and normalized by the standard error. The second measure, increase node purity (the reduction in after split), is similar to that for CART and was computed based on the data used to grow the trees. The difference from the measure for CART is that the value of increase in node purity for RF is averaged from all the trees and the value is not scaled to 100%.

As ensemble learning methods, CART and RF allow us to analyze both categorical data and continuous data simultaneously and have alternative ways to deal with missing data. In contrast to RF, CART is not so sensitive to missing data. It can produce reasonable results with high explained variance even without padding missing data. However, CART is less robust, since a small change in the data can cause a large change in the estimated final tree (James et al., 2013). The performance can be substantially improved by RF aggregating of thousands of decision trees. Thus, CART and RF are complementary in their unique strengths and weaknesses, and the results generated from the two models can be used for cross-validation.

2.3.3. Correlation and regression analysis

CART and RF were used to identify the main controlling factors for MFV. However, the exact relationships between MFV and the controlling factors are not determined by the methods because CART and RF are non-parametric methods. The correlation analysis method was used to analyze the individual relationships between MFV and each of the controlling factors. Once the controlling factors were narrowed down to those with statistically significant relationships with MFV, stepwise regression was applied to further select the controlling factors as the predictive variables of MFV in the format of empirical formula. Adding or removing predictive variables was based on a statistical test (*t*-test) at significance levels of 0.05 and 0.1, respectively. For the *t*-test, the values of MFV were assumed to follow a normal distribution after a logarithmic transformation.

3. Results

3.1. Statistics of MFV

Across all measurements at three spatial scales, MFV is found in the range of 2.22×10^{-5}~1.83×10^{-1} $m\ s^{-1}$. Considering the range of MFV over four orders of magnitude, the geometric mean is used to express

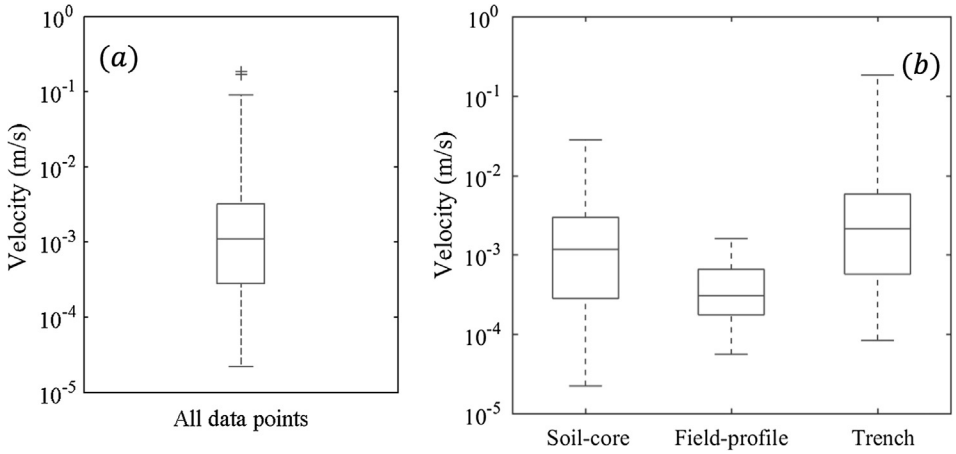

Fig. 1. Typical values and ranges of measured macropore flow velocity (MFV) (a) for all data points and (b) data points at different observation scales.

the mean value of MFV (Nimmo, 2007), which is $1.08 \times 10^{-3}\ m\ s^{-1}$ (Fig. 1). On average, the largest MFV values occur at the trench scale and the smallest at the field-profile scale. In terms of geometric mean, the MFV value at the trench scale is 6.0 and 2.1 times larger than those at the field-profile scale and soil-core scale respectively. Note that the difference among the MFV values at the three scales is statistically significant ($p < 0.01$, t-test).

The MFV differences across scales can be mostly attributed to the differences in the structures of the macropores. First of all, the trench-scale experiments were conducted on hillslopes where abundant macropores exist with large diameter generated by decayed or alive roots, earth worms, and even subsurface erosion (Beven and Germann, 1982). In the soil-core scale experiments, the probability of incorporating large macropores into a core decreases with core sampling scale (Allaire et al., 2009), which is around 20 cm in the studies examined, so there is a low probability that the core contains obvious large macropores. Secondly, geometric mean of MFV at soil-core scale is larger than that at field-profile scale. This can be attributed to the connectivity of macropore network. In fact, as individual macropore length is small (usually less than 25 cm (Sidle et al., 2001)), soil-core scale with smaller travel distance (18 cm on average) corresponds to a better connected macropore network and thus larger MFV compared to field-profile scale with longer travel distance (82 cm on average). Thirdly, the measured MFV values at the trench scale are largely dominated by lateral macropore flow, while those measured at the field-profile and soil-core scales are dominated by vertical macropore flow. Cheng et al. (2017) suggested that macropore diameters in the lateral direction are generally larger than those in the vertical direction.

Moreover, the MFV values derived from the MF measured from single macropores are the largest across all data points, i.e., no less than $7 \times 10^{-3}\ m/s$ (see the upper whisker of boxplot in Fig. 1(a)). This is because measuring individual macropore discharge is only possible when the macropore diameter is large enough to be measurable.

MFV values are not easy to be obtained and not extensively available. On the other hand, K_s values can be approximated based on soil property data (such as sand, clay and silt fractions) which are extensively available. Therefore, if a ratio can be identified between MFV and K_s, it will be convenient to estimate MFV a priori before calibrating a catchment hydrologic model. Although the ratio of MFV and K_s varies over 7 orders of magnitude for all data points, its 25th and 75th percentiles are within 2 orders of magnitude ranging from 29 to 2450 (Fig. 2). The geometric mean of the ratios for all data points is 339, and for the three scales (trench, field-profile, soil-core), it is 3099, 132, and 49, respectively. This means MFV is about 2 ~ 3 orders larger than the corresponding values of saturated hydraulic conductivity. At the trench scale, the ratio is much larger than those at the field-profile and soil-core scales; this is reasonable since here K_s is assumed to be isotropic whilst the trench-scale MFV values are more dominated by lateral MF which tends to be faster than the vertical MF due to a more efficient macropore network (Zehe et al., 2010).

3.2. Dominant controlling factors of MFV

3.2.1. Controlling factors identified by CART and RF

The regression tree for MFV generated from CART is shown in Fig. 3. Here the complexity parameter is set as 0.025, i.e., each splitting step must increase R^2 by at least 0.025. The tree starts with whether the observation scale is the trench scale or not. At the trench scale, macropore diameter is the first control on MFV. Larger macropore diameters ($D > 100$ mm) are associated with larger MFV. For the soil-core and field-profile scales, these data points are split according to whether the travel distance is greater than 19 cm. Short travel distance corresponds to large MFV. The overall variance explained by the regression tree is 57.1%.

According to the regression tree, the three most important variables for explaining MFV are *Scale*, *L*, and *D* (Fig. 4(a)). The R^2 value for the training data increases with the numbers of splits. However, the maximum R^2 (0.53) occurs at the third split for cross-validation with 10-fold cross-validation used (Fig. 4(b)). This means that the first three splits are sufficient to explain the variance of observed MFV by *Scale*, *L*, and *D*. Generally, *Scale* is the first-order controlling factor for all data points. *L* is the main controlling factor at soil-core and field-profile scales and *D* is the dominant factor for MFV at trench scale.

For the RF model without padding the missing data, the explained variance of random forests is very low and the increase in MSE can be negative if missing data are not dealt with. Thus, it is necessary to replace missing data first. For continuous predictors, one option is the weighted average of the non-missing observations, where the weights are the proximities. There are alternatives. For many observations conducted under ponding conditions with sufficient water supply at the soil-core scale, the rate of water infiltration into the soil is equal to or greater than K_s. Hence, it is reasonable to replace the missing values of rainfall intensity by the value of K_s. The macropore diameter is usually small at the soil-core and field-profile scales. If the replaced values of *D* are larger than 5 mm, they are set as the mean observed values at the two scales (about 2.8 mm). After these replacements, the explained variance is 63.4%.

Considering the measures of variable importance, increase in MSE and increase in node purity, *D*, *I* and *L* are ranked as the top three most important variables (Fig. 5). Compared to the results from CART, *D* and *L* are both identified as important variables, while now *I* becomes important instead of *Scale*. The reason for this may be that, after padding,

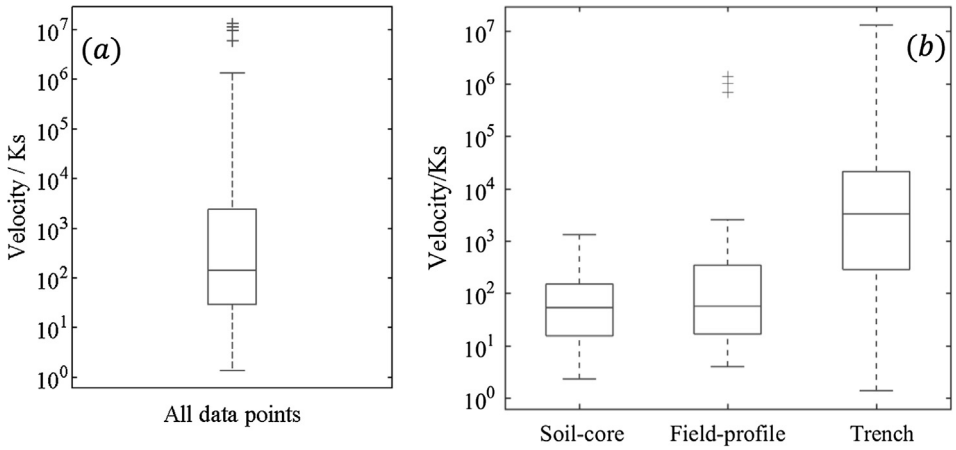

Fig. 2. Ranges of the ratio of macropore flow velocity (MFV) and saturated hydraulic conductivity (K_s) (a) for all data points and (b) data points at different observation scales.

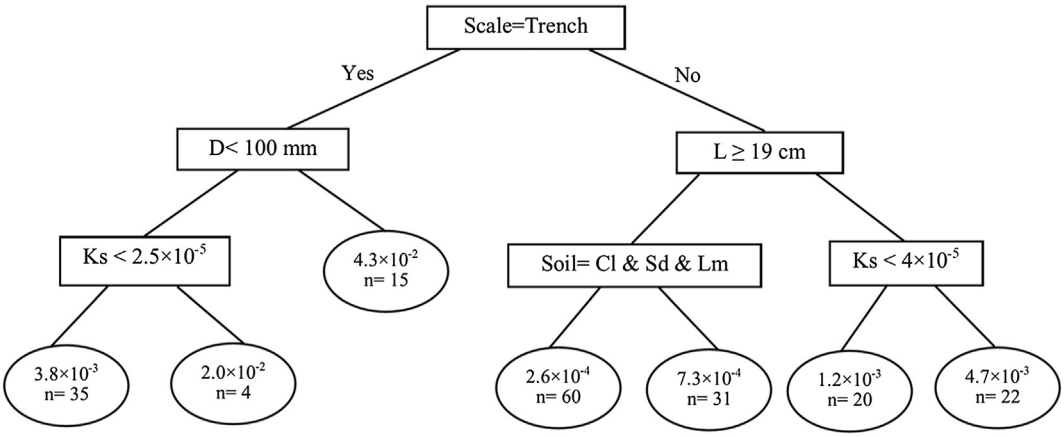

Fig. 3. Decision tree for MFV generated from CART. The ellipses are the leaves of the tree and contain the geometric mean values (unit: m/s) and the number of MFV collected in each leaf. The rectangles contain the identified predictors. All branches leaving the rectangles from the left (right) correspond to outcomes when the statement in the rectangle is TRUE (FALSE). For symbols see text.

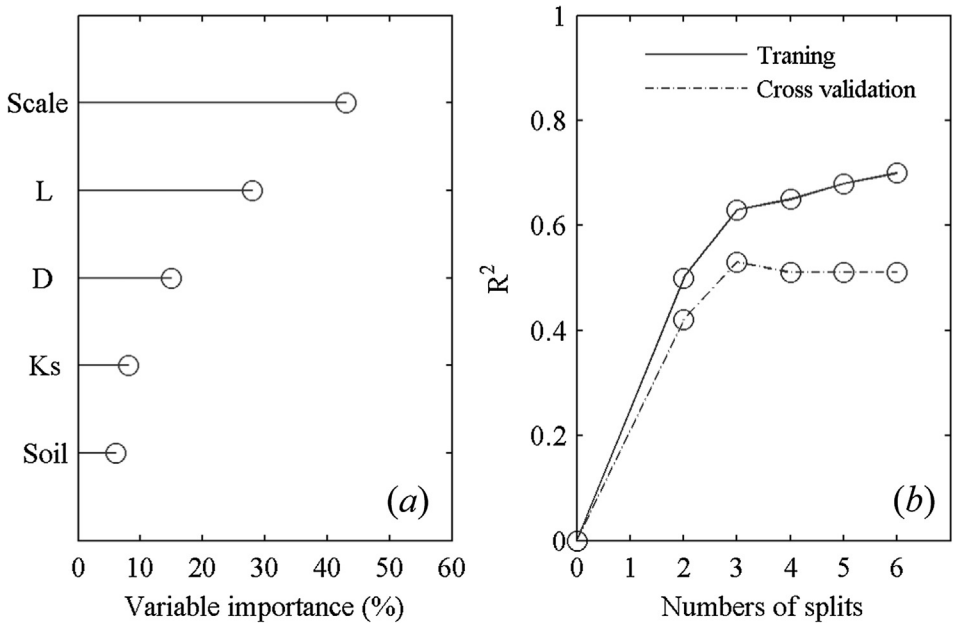

Fig. 4. (a) Predictor variable importance determined from CART and (b) the coefficient of determination, R^2, versus the number of splits for training and cross-validation data. For symbols see text.

D at the trench scale is much larger than that at the field-profile and soil-core scales while, after padding, *I* at the soil-core scale is also larger than that at the trench and field-profile scales. Hence the large difference of *D* and *I* among the scales may dominate over the influence of *Scale* as an important controlling factor.

3.2.2. Correlation analysis for controlling factors and MFV

Based on the results from CART and RF, *Scale*, *L*, *D*, and *I* are identified as the dominant controlling factors on MFV. The effect of *Scale* on MFV has been discussed in Section 3.1. Observed values of *D* are mainly available at the trench scale but less so at the other two scales. In this subsection we conduct a correlation analysis across all scales to elucidate the explicit relationships between MFV and the other two identified controlling factors (*L* and *I*). The effects of other factors like soil texture and land use are also examined.

MFV and travel distance have significantly positive correlation considering all data points (Fig. 6). However, this positive correlation only holds at the field-profile scale. At the trench scale, MFV and *L* are uncorrelated, whereas a significant negative correlation is detected at the soil-core scale. Recall the regression tree analysis shown in Fig. 3, there is a splitter with $L = 19$ cm for the soil-core and field-profile scales, where smaller *L* corresponds to larger MFV. This suggests a non-linear relationship between *L* and MFV. If the data of the soil-core and field-profile scales are pooled, MFV decreases with *L* when *L* is smaller than 19 cm, but it tends to increase with *L* for larger values of *L*.

The non-linear relationship between *L* and MFV at soil-core and field-profile scales may be attributed to the connectivity of the macropore network. At the soil-core scale, the length of individual macropores is usually less than 25 cm (Sidle et al., 2001). The inverse relationship between MFV and *L* (Fig. 6b) suggests that macropore networks may be better connected at short travel distances, leading to faster MFV. For example, the mean value of MFV calculated from Bodhinayake and Si (2004) was 1.26×10^{-5} m/s with relatively longer travel distance ($L = 20$ cm), while the MFV value calculated from Rawls et al. (1993) was much larger ($V = 9.30 \times 10^{-3}$ m/s) with shorter travel distance ($L = 5 \sim 6$ cm). Considering the macroporosities from the former experiments were about 27 times larger than the latter ones, it indicates the macropore network with shorter travel distance has much better connectivity. The inverse relationship between MFV and *L* is also consistent with the findings of Koestel et al. (2012), who performed a

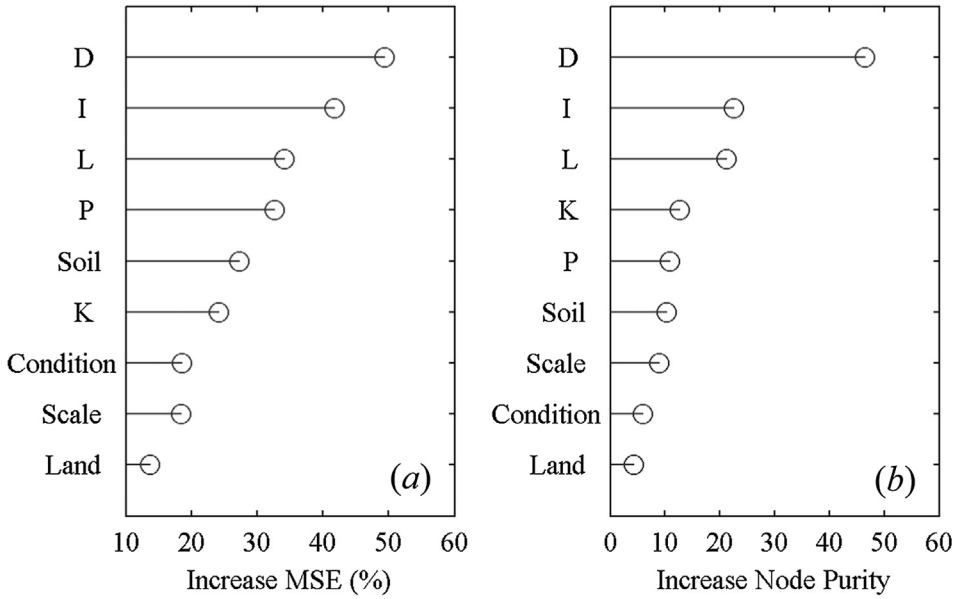

Fig. 5. (a) Mean increase in MSE (Mean Square Error) and (b) mean increase in node purity of predictor variables from the random forests model. For symbols see text.

meta-analysis using the normalized first 5% arrival-time of the breakthrough curve as a proxy of macropore flow at the soil-core scale. At the field-profile scale, much larger macropores can be present as travel distance increases, which offset the negative effect of macropore network connectivity. At the trench scale, field measurement results seem to be more site-dependent, so the correlation between L and MFV is weak (Anderson et al., 2009b; McGuire et al., 2007; Megahan and Clayton, 1983; Wienhöfer et al., 2009). That is, the observed MFV may be more dependent on whether the experimental site features any highly connected preferential flow network (Anderson et al. 2009b), so the travel distance may not reflect the connectivity of the macropore network or macropore diameter at trench scale. The positive correlation found when all data points are analyzed may result from the larger MFV values at the trench scale as water travels longer distances compared to the field-profile and soil-core scales.

Rainfall intensity I represents the boundary condition of the experiments. MFV has a significantly positive correlation with I for all data points and at all three scales (Fig. 7), indicating that MFV is a dynamic variable instead of a static property of specific sites. As I increases, more water enters into and flows through the macropores and this tends to increase the hydraulic connectivity within the macropore network (Sidle et al., 2000). As a result, it reduces the impacts of friction from the macropore surface on the flow, leading to increased MFV. The positive correlation is also confirmed by site-based experiments (Anderson et al., 2009b; Hincapié and Germann, 2009) and other meta-analyses of preferential flow velocity at the soil-core scale (Koestel et al., 2012).

Regarding the influence of land use, three major types of landuse are considered: forested sites, grasslands and farmlands. The geometric mean value of MFV from forested sites is slightly larger than that from grasslands, and obviously larger than that from farmlands (Fig. 8(a)). The difference of MFV among land use types is statistically significant ($p < 0.01$, t-test). This observation is consistent with previous studies according to which (1) the diameters of macropores are generally larger in forested areas than grasslands due to more active root dynamics and earthworm activities (Alaoui et al., 2011); (2) agriculture cultivation in farmlands tends to destroy the macropore and reduce the connectivity of macropore in the top soils (Lindahl et al., 2009). Regarding the impacts of soil texture, no significant difference was identified in general ($p > 0.05$, t-test). Although the median MFV values are somewhat different among different soil textures, the ranges of MFV are similar for different soil textures (Fig. 8(b)).

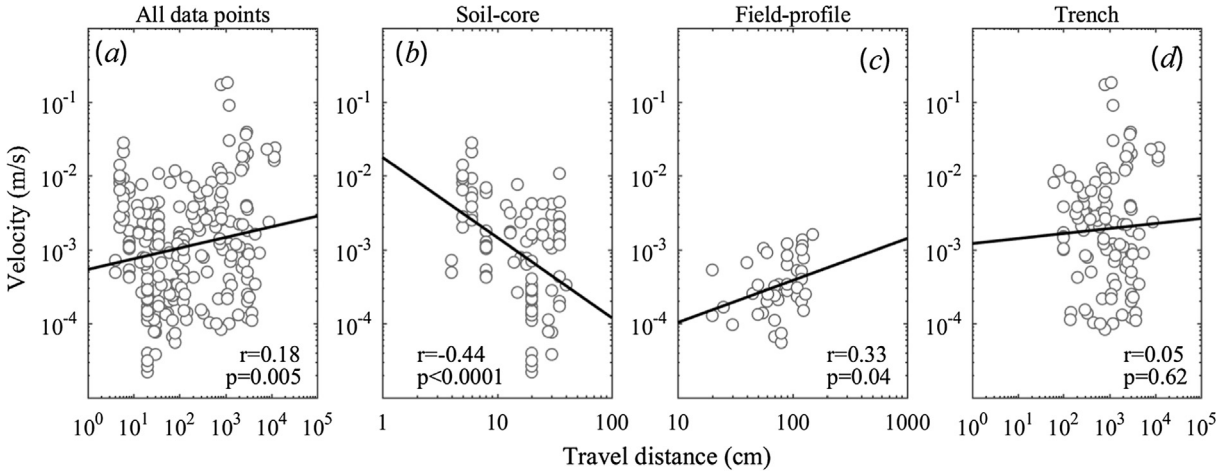

Fig. 6. Relationships between MFV and travel distance (L) for (a) all data points, and data points at (b) soil-core scale, (c) field-profile scale, and (d) trench scale.

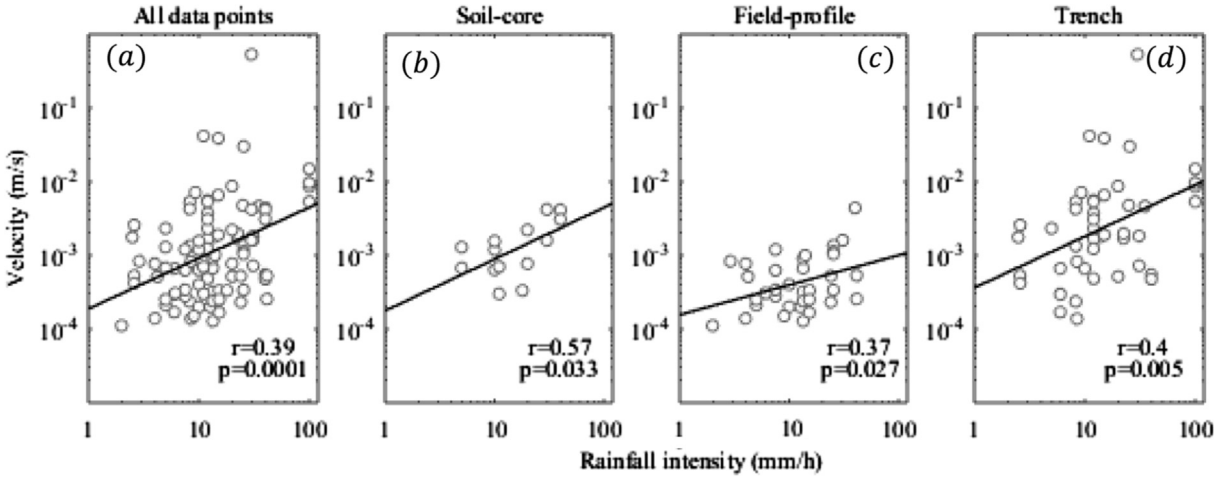

Fig. 7. Relationships between MFV and rainfall intensity (I) for (a) all data points, data points at (b) soil-core scale, (c) field-profile scale, and (d) trench scale.

3.3. Estimating MFV with multi-variate regression

Since trench-scale MFV measurements are more relevant to processes at hillslope-to-catchment scales, we further analyze the trench-scale results to develop empirical relationships that may be useful for hydrologic modeling of hillslopes and catchments.

3.3.1. New empirical formula to estimate MFV

In CART and RF, D, as an indicator of macropore morphology, has been identified as a dominant control at the trench scale (Fig. 3). D is used as a criterion to divide the data into two groups, to which correlation and regression analyses are applied to analyze the relationship between site factors and MFV.

The splitting value of D derived from CART is only helpful for analysis of data with measured D, because the partition at trench scale (Fig. 3) does not account for missing data that make up 46% of the data points at the trench scale. Thus, the splitting value generated from CART is not adopted here. Instead, data points with $D > 10\ mm$ are classified as large macropore group (55 data points), and data with $D < 10\ mm$ or data with no information on the size of macropore diameter are classified as small macropore group (55 data points). The MFV values of larger macropore are 6 times larger than those of small macropore (Fig. 9), and this difference is statistically significant (p-value < 0.01, t-test).

For the large macropore group, MFV shows significantly positive correlations with I and D (Fig. 10). Larger I and D correspond to faster MFV. The significantly negative correlation between slope gradient (S) and MFV, however, seems counterintuitive. The negative correlation

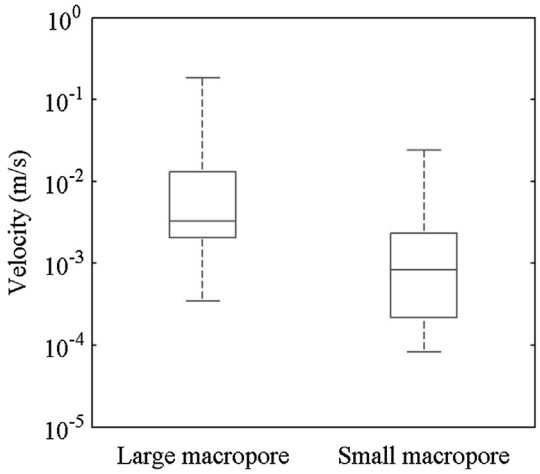

Fig. 9. The effect of macropore diameter for the large macropore group (diameter < 10 mm) and small macropore group (diameter < 10 mm or without information on macropore size) on MFV at the trench scale.

results from a significantly negative correlation between S and D. The partial correlation between MFV and S is positive ($r = 0.32$, $p = 0.23$) after removing D. Other factors like the travel distance L or mean annual precipitation P are not significantly correlated with MFV. Based on the above discussion, the MFV values in the large macropore group can be well predicted by a multivariate regression formula (Fig. 11(a)), with rainfall intensity and macropore diameter as the major explanatory

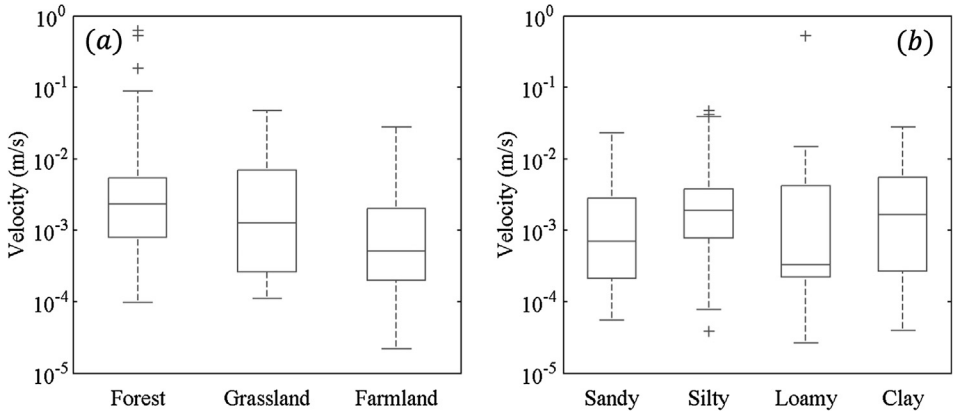

Fig. 8. The effects of (a) land use and (b) soil texture on MFV.

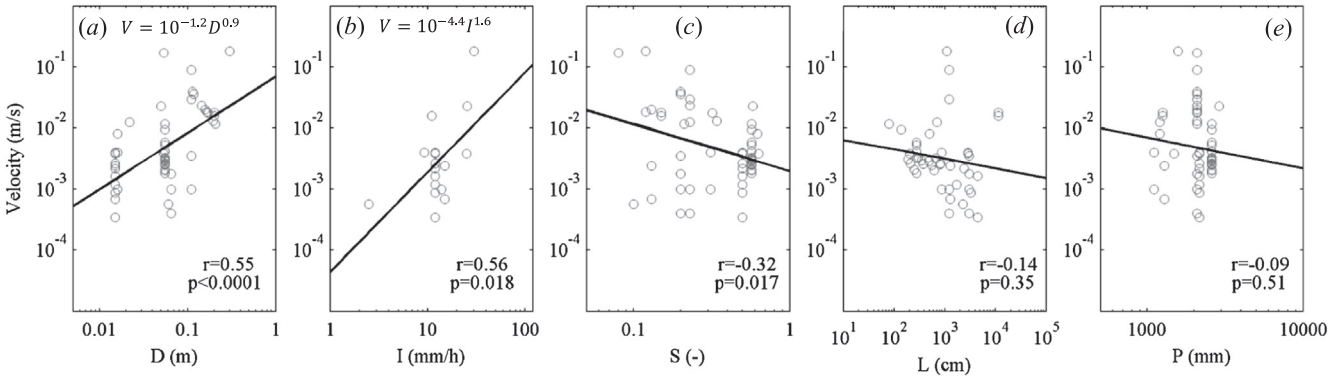

Fig. 10. The relationships of MFV with (a) macropore diameter (D), (b) rainfall intensity (I), (c) slope gradient (S), (d) transport distance (L) and (e) mean annual precipitation (P) at the trench scale for the large macropore group.

factors. Rainfall intensity can be regarded as a proxy of the filling degree of macropore. Larger rainfall intensity indicates a greater filling degree of macropores. This regression formula indicates that MFV is mostly determined ($R^2 = 0.76$) by the rainfall property (rainfall intensity, I), and the intrinsic macropore morphology (macropore diameter, D):

$$V = 0.0184\left(\frac{D}{4}\right)^{1.02} I^{1.27} \tag{2}$$

One may notice there are indeed more data points in Fig. 11b than those in Fig. 11a. It is because the multiple regression in Fig. 11a requires the experiments contain information of both rainfall intensity and macropore diameter, while data points in Fig. 11b only need information on macropore diameter.

3.3.2. Comparison with existing equations of MFV estimation

In literature, there are theoretical equations, i.e. Poiseuille equation and Manning equation, usually used to estimate MFV primarily. Comparing the regression formula derived from field measurements with these existing equations could provide some insight into the possible limitations of these theoretical equations and the implications of other potential controlling factors.

The Poiseuille equation, with the hypothesis that the MF flow regime is dominated by laminar flow (Šimůnek et al., 2003), is one of the most popular equations. It can be expressed as

$$V = \frac{D^2}{32}\frac{g}{\nu}S_f \tag{3}$$

where ν is the kinematic viscosity that is equal to 1.0×10^{-6} (m^2/s) at 20 °C, g is gravity acceleration and S_f is hydraulic gradient. Based on the Poiseuille equation, the estimated MFV values can be several orders of magnitude larger than those presented in Section 3.1. For example, when the macropore diameter equals to 2 mm, the estimated MFV for a vertical profile can be as large as 1 m/s, which is 3 orders of magnitude larger than the geometric mean value of the measured MFV. This order of magnitude difference between the Poiseuille equation and MFV measurements suggest that laminar flow may not be a good assumption for MF in the experiment sites.

The Manning equation, assuming that the MF flow regime is dominated by turbulent flow, is another frequently used equation. The equation is expressed as:

$$V = \frac{1}{n_f} R_H^{2/3} S_f^{1/2} \tag{4}$$

where n_f is roughness coefficient ranging from 0.016 to 0.14 for soil material surface (Chow, 1959). According to the Manning equation, MFV decreases with n_f. The Manning equation also tends to overestimate MFV even by setting n_f as upper limit 0.14. As the inner wall surface of macropores may exert more friction force to water than the upper soil surface (Chen and Wagenet, 1992), we calibrated the n_f value here to achieve the best predicting power. The resulted n_f value is 7.0 (Fig. 11(b)), much higher than the typically recommended range for soil surfaces. Even so, the coefficient of determination (R^2) is only 0.16 (Fig. 11(b)), much lower than that from our regression formula.

Both theoretical equations for laminar flow (Poiseuille equation)

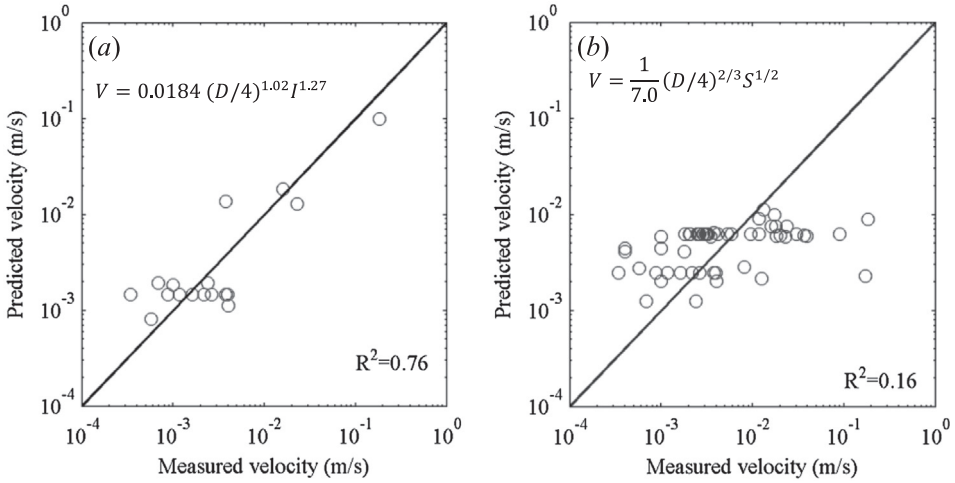

Fig. 11. Measured vs. predicted macropore flow velocity values (a) from multiple regression equation and (b) by Manning's equation at the trench scale for the large macropore group.

and turbulent flow (Manning equation) could not provide a reasonable estimation of MFV. There are two main reasons that may explain the overestimation of MFV. The first reason is related to the filling degree of macropores. Since macropores are buried beneath ground, the filling degree of macropores is mostly unknown during the experimental period. Fig. 7 shows that MFV is a dynamic variable depending on the rainfall intensity, which controls the water content in macropores. It is very likely that the macropores are only partially filled with water. In the Manning equation (Eq. (4)) R_H is estimated as $D/4$ which only holds when the macropores are fully filled by water, which may rarely occur in reality. In other words, R_H is likely overestimated in the first place. The calibrated value of n_f is much higher than the typical range, implying that the value is adjusted to compensate for the effects from overestimation of R_H. On the other hand, the effective roughness of the macropore inner wall is generally much larger when the macropores are partially filled than when they are fully filled.

Secondly, the connectivity of the macropore network is not reflected in the Poiseuille and Manning equations, which are originally derived for individual pipes or macropores. Individual macropores are small and their length is usually under 25 cm (Sidle et al., 2001). A macropore network is composed of a number of individual macropore pipes which themselves are disconnected most of the time. The flow from one macropore may have to penetrate the soil matrix before getting into another adjacent macropore. In overcoming the obstruction of the soil matrix, much energy is dissipated, and the flow velocity is reduced. Wienhöfer et al. (2009) noted that the spatial arrangement and internal connectivity of the preferential network constitute the first-order controls on the hydrological response of hillslopes. Besides, the connectivity of the macropore network is dynamic (Guo et al., 2014). As the soil is wetted, more macropores are activated and the connectivity of the macropore network increases. As water tends to follow the least resistant flow path (Sidle et al., 2001; Weiler and McDonnell, 2007), the resistance of the macropore network is also a function of soil moisture content and water supply.

These analyses suggest that including the effects of the filling degree of macropore and the roughness of macropore network is of great importance in estimating MFV. Here we suggest that rainfall intensity can act as a proxy for the filling degree of macropore (Fig. 11(a)). A parameter reflecting the connectivity of the macropore network is also necessary to be introduced to equations for estimate MFV in soils.

4. Discussion and conclusion

4.1. Discussion

4.1.1. Comparison to MFV statistics from other studies

The statistics of MFV have been summarized in a few studies. Nimmo (2007) collected 64 field tests of preferential flow at the field-profile scale and found that the maximum transport velocity has a geometric mean of $1.5 \times 10^{-4}\ m/s$, which is much smaller than the geometric mean value for all data points found in this study, and twice as small as the geometric value at the field-profile scale in this study (see Section 3.1). One possible reason is that Nimmo (2007) considered both MFV in soils and rocks and generally MF is slower in rocks. What's more, Nimmo (2007) focused on preferential flow, which includes both macropore flow and other flow types, i.e. finger flow and funnel flow. Uchida et al. (2001) summarized the observed velocities in soil pipes from nine studies which were on the order of 5.4×10^{-3}~$8 \times 10^{-1}\ m/s$, i.e., at the upper end of the MFV values at the trench scale, which is reasonable since the macropore diameters involved in the studies cited by Uchida et al. (2001) are relatively large. In our study, we used a much larger dataset that contains 243 experimental data points, so the typical values and general range of MFV provided here are more representative for soils.

4.1.2. Comparison to controlling factors of MFV identified in other studies

In our study, observation scale, travel distance, rainfall intensity, and macropore diameter are identified as the most important factors that control MFV. Compared to other studies using data from experiments at the soil-core scale or field-profile scale only, our study covers three scales, which allows observation scale and travel distance to be identified as major controls.

As a macropore morphological factor, macropore diameter is included and has been identified as a key factor in determining MFV, especially at the trench scale. Several studies have emphasized the importance of macropore diameter in determining MFV. Smettem and Collisgeorge (1985) showed that MFV has a power-law relationship with pore diameter in the range of 2~6 mm at soil-core scale. Uchida et al. (2001) also showed a power-law relationship using observations at the trench scale. The Poiseuille and Manning equations for pipeflow have been applied to represent flow velocity in macropores (Chen and Wagenet, 1992) and macropore diameter is a key factor in both equations. Thus, it is reasonable that macropore diameter has been identified as a dominant control.

Rainfall intensity has also been recognized as a proxy of the filling degree of macropores. For example, Anderson et al. (2009b) found that MFV is dependent on the 1-h rainfall intensity and Germann and Beven (1985) modelled MFV as a function of water content in macropore. Further, Germann et al. (2007) derived an equation to calculate MFV based on the Stokes flow theory by treating MFV as a function of film thickness, which is mainly determined by rainfall intensity.

As to the connectivity of the macropore network, several studies have mentioned its importance to determine MFV (Sidle et al., 2001; Weiler and McDonnell, 2007; Wienhöfer et al., 2009), but no equations describing MFV have accounted for such effect to our knowledge. In order to do this, the connectivity of the macropore network and its influence on MFV must be well represented. Despite difficulties, some efforts have been undertaken to address this problem. At the soil-core scale, a macropore network can be visualized by X-ray computed tomography and the properties of connectivity can be estimated (Naveed et al., 2016). At the field-profile scale, Weiler and Naef (2003) used dye tracer to examine the interaction between the soil matrix and the macropore network, which reflects the connectivity of macropore network. At the trench scale, some studies were also conducted to quantify the macropore network accompanying hillslope excavation (Anderson et al., 2009a). This approach is rather expensive, but more importantly, it cannot directly measure the continuity of the macropore network. Recently, Guo et al. (2014) proposed a new practical and non-destructive approach to map the subsurface lateral preferential flow network by ground-penetrating radar. Although the spatial distribution of the macropore network is complex and its activation depends on water moisture conditions, the activated macropore network becomes self-organized as soil moisture increases (Sidle et al., 2000) and it develops based on the path of lowest resistance (Weiler and McDonnell, 2007). Thus, the skeletal macropore network derived from ground-penetrating radar may plausibly capture the connectivity and resistance of the macropore network, and ultimately inform parameterizations of MF in hydrological models.

4.1.3. Controlling factors of other MF attributes

MFV is a key attribute of MF but it is only meaningful when MF does occur. Several studies have looked at other attributes of MF, such as the strength of MF (quantified by different indicators, the relative 5%-arrival time of inert tracer (Koestel and Jorda, 2014)) and the occurrence of MF. These attributes need to be considered simultaneously when modeling MF process. It is meaningful to synthetically compare the similarity and dissimilarity of controlling factors between MFV and other MF attributions.

Overall, the strength of MF is mainly related to soil texture and the occurrence of MF is largely controlled by the boundary conditions, i.e. rainfall properties. Considering the strength of MF, several studies

showed that clay content is a key controlling factor, i.e., larger clay content tends to produce larger degree of MF (Jarvis et al., 2009; Koestel et al., 2012; Koestel and Jorda, 2014). Other controlling factors were also investigated previously. For example, Koestel et al. (2012) found that the degree of preferential flow decreases with travel distance; Koestel and Jorda (2014) suggested that information on the water saturation state is important for better prediction of MF.

As to the occurrence of MF, rainfall properties are usually considered as essential controlling factors. Liu and Lin (2015) found that MF tends to occur more frequently in response to intense rainfall events. Peng et al. (2016) showed that rainfall amount is the prominent control on the occurrence of MF. Wiekenkamp et al. (2016) indicated that MF is triggered by both amount and intensity of rainfall. Heppell et al. (2002) categorized rainfall-induced MF into intensity-driven and duration-driven types. Lastly, antecedent soil moisture and topography also have noticeable impacts on the occurrence of MF.

4.1.4. Implications for further research

Generally, the factors affecting MF can be grouped into macroscopic and microscopic factors. Land use, soil texture, observation scale, travel length, climate (precipitation), and rainfall intensity are macroscopic factors, while macropore diameter, macroporosity, macropore continuity, and macropore network connectivity are microscopic factors. Theoretically, MFV could be directly determined by the microscopic factors when the water supply conditions are known. The macroscopic factors reflect or control the microscopic characteristics in an indirect way. This statement also applies to the strength of MF, which is mainly determined by the density and macroporosity of MF (Jarvis et al., 2009). The clay content related to the generation of cracks and fissures reflects some of the microscopic factors. Thus, finding appropriate macroscopic factors reflecting microscopic properties controlling MFV is a potential way of estimating MFV.

Other factors such as antecedent soil moisture (Nimmo, 2012) may also be necessary for inclusion in future studies. Higher soil moisture will facilitate the movement of water from the soil matrix to the macropore and lessen the resistance of the macropore network (Sidle et al., 2000), which will trigger rapid macropore flow response and fast velocity at a certain rainfall intensity.

4.2. Conclusions

According to our meta-analysis, the observed MFV values range between 2.22×10^{-5}~1.83×10^{-1} $m\ s^{-1}$. The geometric mean is 1.08×10^{-3} $m\ s^{-1}$, which is about 2~3 orders of magnitude larger than the corresponding value of saturated hydraulic conductivity of the soil matrix. MFV values and the ratios of MFV to K_s are significantly different across scales. MFV at the trench scale is 3 ~ 10 times larger than that MFV at the soil-core and field-profile scales. The ratio of MFV to K_s at the trench scale is 23 and 62 times that at the soil-core and field-profile scales, respectively.

Observation scale, travel distance, macropore diameter and rainfall intensity are identified as major controlling factors for MFV by the CART and RF analyses, with the total variance explained reaching around 60%. However, neither soil texture nor land use shows significant influence. Generally, MFV increases with travel distance considering all data points. A non-linear relationship exists between MFV and travel distance because MFV decreases with travel distance at the soil-core scale but correlation at the trench scale is nonsignificant. MFV depends on rainfall intensity at all scales. At the same time, macropore diameter is regarded as the first-order control at the trench scale, and larger macropores tend to be associated with larger MFV values. Combining information of macropore diameter and rainfall intensity, MFV can be predicted by a multivariate regression equation with accuracy ($R^2 = 0.76$) at the trench scale. In contrast, the Poiseuille or the Manning equations do not predict MFV well, which suggests that it is important to consider the degree of macropore saturation by a proxy such as rainfall intensity. The results also point to the need of introducing a parameter to represent the effect of macropore network connectivity on MFV.

Although our findings are still preliminary, they suggest a potential for better estimating MFV using local site factors. More experiments combining measurements of saturated and unsaturated hydraulic conductivity, MFV, and potential controlling factors at diverse scales are needed to explore their relationships within and across scales. Investigating the relationships between macroscopic factors and microscopic factors (e.g., macropore morphology and macropore network connectivity) on MFV is also of great value to infer MFV by using readily accessible site factors.

Acknowledgement

This research was supported by the Office of Science of the U.S. Department of Energy through the Energy Exascale Earth System Modeling (E3SM) project of Earth System Modeling program. Contributions by L.R. Leung and X. Chen were supported by the Next Generation Ecosystem Experiment (NGEE) Tropics project of Terrestrial Ecosystem Systems program and the River Corridor and Watershed Hydrobiogeochemistry Scientific Focus Area of Subsurface Biogeochemical Research program, respectively. PNNL is operated for DOE by Battelle Memorial Institute under contract DE-AC05-76RL01830. The meta-data used in this study are available upon request to the corresponding author Hong-Yi Li at hongyili.jadison@gmail.com.

Appendix

Table A. Sources and conditions of the dataset used in this study.

Study	Data points	Scale	Method	Land cover	Location
Anderson et al. (2009a)	9	Trench	Macropore discharge	Forest	Canada (British Columbia)
Anderson et al. (2009b)	16	Trench	Tracer	Forest	Canada (British Columbia)
Beasley (1976)	1	Trench	Rainfall-Runoff lag	Forest	USA (Mississippi)
Buttle et al. (2002)	2	Trench	Tracer	Forest	Canada (Ontario)
Cheng et al. (2009)	1	Trench	Macropore discharge	Forest	China (Hubei)
Feyen et al. (1999)	4	Trench	Tracer	Forest	Switzerland
Graham et al. (2010)	18	Trench	Tracer	Forest	New Zealand
Jackson et al. (2016)	2	Trench	Tracer	Forest	USA (South Carolina)
Joerin et al. (2005)	2	Trench	Tracer	Forest	Switzerland
Kienzler and Naef (2008)	4	Trench	Tracer	Grassland	Switzerland
Kitahara (1993)	2	Trench	Tracer	Forest	Japan (Hokkaido)

Laine-Kaulio et al. (2014)	1	Trench	Tracer	Forest	Finland
Lange et al. (2015)	1	Trench	Tracer	Forest	Mongolia
McCaig (1983)	1	Trench	Tracer	Grassland	UK (Yorks)
McDaniel et al. (2008)	1	Trench	Tracer	Grassland	USA (Idaho)
McGuire et al. (2007)	2	Trench	Tracer	Forest	USA (Oregon)
Megahan and Clayton (1983)	4	Trench	Tracer	Forest	USA (Idaho)
Mehlhorn et al. (1998)	1	Trench	Tracer	Forest	Germany
Mikovari et al. (1995)	4	Trench	Tracer	Forest	Germany
Mosley (1979)	3	Trench	Tracer	Forest	New Zealand
Mosley (1982)	4	Trench	Rainfall-Runoff lag	Forest	New Zealand
Noguchi et al. (1999)	1	Trench	Tracer	Forest	Japan
Nyberg et al. (1999)	3	Trench	Tracer	Forest	Sweden
Retter et al. (2006)	2	Trench	Tracer	Grassland	Switzerland
Schneider et al. (2014)	2	Trench	Tracer	Forest	Switzerland
Tanaka et al. (1988)	1	Trench	Tracer	Forest	Japan
Tromp-van Meerveld and McDonnell (2006)	2	Trench	Tracer	Forest	USA (Georgia)
Tsuboyama et al. (1994)	2	Trench	Macropore discharge	Forest	Janpan
Uchida et al. (1999)	1	Trench	Macropore discharge	Forest	Japan
Weiler et al. (1998)	4	Trench	Tracer	Forest	Switzerland
Weiler and McDonnell (2007)	1	Trench	Tracer	Forest	New Zealand
Wienhöfer et al. (2009)	8	Trench	Tracer	Forest	Austria
Angermann et al. (2017)	1	Field-profile	No-sequence response	Forest	Luxembourg
Aubertin (1971)	4	Field-profile	Tracer	Forest	USA (Ohio)
Cey and Rudolph (2009)	2	Field-profile	Tracer	Agriculture	Canada (Ontario)
Cullum (2009)	1	Field-profile	Tracer	Agriculture	USA (Mississippi)
Everts and Kanwar (1990)	2	Field-profile	Tracer	Agriculture	USA (Iowa)
Frey et al. (2012)	1	Field-profile	Tracer	Agriculture	Canada (Ontario)
Hallard and Armstrong (1992)	1	Field-profile	Tracer	Grassland	UK
Hardie et al. (2011)	5	Field-profile	No-sequence response	Agriculture	Australia
Hardie et al. (2013)	3	Field-profile	No-sequence response	Agriculture	Australia
Jaynes et al. (2001)	1	Field-profile	Tracer	Agriculture	USA (Iowa)
Klaus et al. (2014)	2	Field-profile	Tracer	Agriculture	Germany
Kung et al. (2000a)	1	Field-profile	Tracer	Agriculture	USA (Indiana)
Kung et al. (2000b)	4	Field-profile	Tracer	Agriculture	USA (NY)
Laubel et al. (1999)	1	Field-profile	Tracer	Agriculture	Denmark
Pilgrim et al. (1978)	1	Field-profile	Rainfall-Runoff lag	Grassland	USA (California)
Peng et al. (2016)	1	Field-profile	No-sequence response	Forest	China (Beijing)
Richards and Steenhuis (1988)	2	Field-profile	Tracer	Agriculture	USA (New York)
Scaini et al. (2017)	3	Field-profile	Tracer	Forest	Luxembourg
Villholth et al. (1998)	2	Field-profile	Tracer	Agriculture	Denmark
Zehe and Flühler (2001)	1	Field-profile	Tracer	Agriculture	Germany
Bodhinayake and Si (2004)	3	Soil-core	HCM	Grassland	Canada (Saskatchewan)
Buczko et al. (2006)	2	Soil-core	HCM	Agriculture	Germany
Casey et al. (1998)	1	Soil-core	HCM	Agriculture	USA (Iowa)
Clothier and Smettem (1990)	2	Soil-core	HCM	Forest	New zealand
Edwards et al. (1979)	1	Soil-core	HCM	Agriculture	Germany
Frey and Rudolph (2011)	6	Soil-core	HCM	Agriculture	Canada (Ontario)
Germann and Beven (1981)	2	Soil-core	HCM	Agriculture	UK (Oxfordshire)
Hincapié and Germann (2009)	10	Soil-core	No-sequence response	Unknow	Unknow
Jacobsen et al. (1997)	4	Soil-core	Tracer	Agriculture	Denmark
Kim et al. (2010)	2	Soil-core	HCM	Agriculture	USA (Missouri)
Kim et al. (2005)	1	Soil-core	Tracer	Forest	USA
Li et al. (2013)	2	Soil-core	HCM	Grassland	China (Inner Mongolia)
Luo et al. (2008)	2	Soil-core	Tracer	Agriculture	USA (Pennsylvania)
Luo et al. (2010)	8	Soil-core	HCM	Agriculture	USA (Pennsylvania)
Messing and Jarvis (1993)	1	Soil-core	HCM	Agriculture	Sweden
Mohanty et al. (1997)	1	Soil-core	HCM	Agriculture	USA (New Mexico)
Paradelo et al. (2016)	1	Soil-core	HCM	Agriculture	Denmark
Rachman et al. (2004)	3	Soil-core	HCM	Grassland	USA (Iowa)
Rawls et al. (1993)	14	Soil-core	HCM	Agriculture	USA (Minnesota and Wisconsin)
Seyfried and Rao (1987)	5	Soil-core	HCM	Agriculture	Costa Rica
Shaw et al. (2000)	13	Soil-core	Tracer	Agriculture	USA (Geogia)
Smettem and Kirkby (1990)	1	Soil-core	HCM	Grassland	Unknown
Udawatta and Anderson (2008)	3	Soil-core	HCM	Agriculture	USA (Missouri)
Wienhöfer et al. (2009)	4	Soil-core	Tracer	Forest	Austria (Vorarlberg Alps)
Zhang et al. (2014)	2	Soil-core	HCM	Agricultural	China (Jiangxi)

Comments: Tracer represents the approach of artificial tracer; HCM is the abbreviation for approach of hydraulic conductivity and macroporosity; no-sequence response represents the approach of non-sequential soil moisture response.

References

Alaoui, A., Caduff, U., Gerke, H.H., Weingartner, R., 2011. Preferential flow effects on infiltration and runoff in grassland and forest soils. Vadose Zone J. 10 (1), 367–377. https://doi.org/10.2136/vzj2010.0076.

Alaoui, A., Rogger, M., Peth, S., Blöschl, G., 2018. Does soil compaction increase floods? A review. J. Hydrol. 557, 631–642. https://doi.org/10.1016/j.jhydrol.2017.12.052.

Allaire, S.E., Roulier, S., Cessna, A.J., 2009. Quantifying preferential flow in soils: a review of different techniques. J. Hydrol. 378 (1–2), 179–204. https://doi.org/10.1016/j.jhydrol.2009.08.013.

Anderson, A.E., Weiler, M., Alila, Y., Hudson, R.O., 2009a. Dye staining and excavation of a lateral preferential flow network. Hydrol. Earth Syst. Sci. 13 (6), 935–944. https://doi.org/10.5194/hess-13-935-2009.

Anderson, A.E., Weiler, M., Alila, Y., Hudson, R.O., 2009b. Subsurface flow velocities in a hillslope with lateral preferential flow. Water Resour. Res. 45.

Beven, K., Germann, P., 1982. Macropores and water flow in soils. Water Resour. Res. 18 (5), 1311–1325. https://doi.org/10.1029/WR018i005p01311.

Beven, K., Germann, P., 2013. Macropores and water flow in soils revisited. Water Resour. Res. 49 (6), 3071–3092. https://doi.org/10.1002/wrcr.20156.

Bodhinayake, W., Si, B.C., 2004. Near-saturated surface soil hydraulic properties under different land uses in the St Denis National Wildlife Area, Saskatchewan. Canada. Hydrol. Process. 18 (15), 2835–2850. https://doi.org/10.1002/hyp.1497.

Breiman, L., 2001. Random forests. Mach. Learn. 45 (1), 5–32. https://doi.org/10.1023/A:1010933404324.

Breiman, L.I., Friedman, J.H., Olshen, R.A., Stone, C.J., 1984. Classification and regression trees (CART). Encyclopedia Ecol. 40 (3), 582–588.

Cey, E.E., Rudolph, D.L., 2009. Field study of macropore flow processes using tension infiltration of a dye tracer in partially saturated soils. Hydrol. Process. 23 (12), 1768–1779. https://doi.org/10.1002/hyp.7302.

Chen, C., Wagenet, R.J., 1992. Simulation of water and chemicals in macropore soils. I. representation of the equivalent macropore influence and its effect on soil water flow. J. Hydrol. 130 (1–4), 105–126. https://doi.org/10.1016/0022-1694(92)90106-6.

Cheng, J., Zhang, H., Zhang, Y., Shi, Y., Cheng, Y., 2009. Effects of preferential flow on soil-water and surface runoff in a forested watershed in China. Frontiers Forest. China 4 (2), 132–139.

Cheng, Y.Y., Ogden, F.L., Zhu, J.T., 2017. Earthworms and tree roots: a model study of the effect of preferential flow paths on runoff generation and groundwater recharge in steep, saprolitic, tropical lowland catchments. Water Resour. Res. 53 (7), 5400–5419. https://doi.org/10.1002/2016wr020258.

Chow, V.T., 1959. Open channel hydraulics. McGraw-Hill, New York.

dos Santos, J.C.N., de Andrade, E.M., Guerreiro, M.J.S., Medeiros, P.H.A., de Queiroz Palácio, H.A., de Araújo Neto, J.R., 2016. Effect of dry spells and soil cracking on runoff generation in a semiarid micro watershed under land use change. J. Hydrol. 541, 1057–1066. https://doi.org/10.1016/j.jhydrol.2016.08.016.

Dusek, J., Vogel, T., Dohnal, M., Gerke, H.H., 2012. Combining dual-continuum approach with diffusion wave model to include a preferential flow component in hillslope scale modeling of shallow subsurface runoff. Adv. Water Resour. 44, 113–125. https://doi.org/10.1016/j.advwatres.2012.05.006.

Germann, P., Helbling, A., Vadilonga, T., 2007. Rivulet approach to rates of preferential infiltration. Vadose Zone J. 6 (2), 207–220. https://doi.org/10.2136/vzj2006.0115.

Germann, P.F., Beven, K., 1985. Kinematic wave approximation to infiltration into soils with sorbing macropores. Water Resour. Res. 21 (7), 990–996. https://doi.org/10.1029/WR021i007p00990.

Guo, L., Chen, J., Lin, H., 2014. Subsurface lateral preferential flow network revealed by time-lapse ground-penetrating radar in a hillslope. Water Resour. Res. 50 (12), 9127–9147. https://doi.org/10.1002/2013wr014603.

Hardie, M., Lisson, S., Doyle, R., Cotching, W., 2013. Determining the frequency, depth and velocity of preferential flow by high frequency soil moisture monitoring. J. Contam. Hydrol. 144 (1), 66–77. https://doi.org/10.1016/j.jconhyd.2012.10.008.

Hardie, M.A., Cotching, W.E., Doyle, R.B., Holz, G., Lisson, S., Mattern, K., 2011. Effect of antecedent soil moisture on preferential flow in a texture-contrast soil. J. Hydrol. 398 (3–4), 191–201. https://doi.org/10.1016/j.jhydrol.2010.12.008.

Heppell, C.M., Worrall, F., Burt, T.P., Williams, R.J., 2002. A classification of drainage and macropore flow in an agricultural catchment. Hydrol. Process. 16 (1), 27–46. https://doi.org/10.1002/hyp.282.

Hincapié, I., Germann, P.F., 2009. Impact of initial and boundary conditions on preferential flow. J. Contam. Hydrol. 104 (1–4), 67–73. https://doi.org/10.1016/j.jconhyd.2008.10.001.

James, G., Witten, D., Hastie, T., Tibshirani, R., 2013. An introduction to statistical learning. Springer, New York.

Jarvis, N., Koestel, J., Messing, I., Moeys, J., Lindahl, A., 2013. Influence of soil, land use and climatic factors on the hydraulic conductivity of soil. Hydrol. Earth Syst. Sci. 17 (12), 5185–5195. https://doi.org/10.5194/hess-17-5185-2013.

Jarvis, N.J., 2007. A review of non-equilibrium water flow and solute transport in soil macropores: principles, controlling factors and consequences for water quality. Eur. J. Soil. Sci. 58 (3), 523–546. https://doi.org/10.1111/j.1365-2389.2007.00915.x.

Jarvis, N.J., Moeys, J., Hollis, J.M., Reichenberger, S., Lindahl, A.M.L., Dubus, I.G., 2009. A conceptual model of soil susceptibility to macropore flow. Vadose Zone J. 8 (4), 902–910. https://doi.org/10.2136/vzj2008.0137.

Jones, J.A.A., 2010. Soil piping and catchment response. Hydrol. Process. 24 (12), 1548–1566. https://doi.org/10.1002/hyp.7634.

Jury, W.A., Gardner, W.R., Gardner, W.H., 1991. Soil physics. John Wiley & Sons, New York.

Koch, J.C., Ewing, S.A., Striegl, R., McKnight, D.M., 2013. Rapid runoff via shallow throughflow and deeper preferential flow in a boreal catchment underlain by frozen silt (Alaska, USA). Hydrogeol. J. 21 (1), 93–106. https://doi.org/10.1007/s10040-012-0934-3.

Koestel, J., Jorda, H., 2014. What determines the strength of preferential transport in undisturbed soil under steady-state flow? Geoderma 217, 144–160. https://doi.org/10.1016/j.geoderma.2013.11.009.

Koestel, J.K., Moeys, J., Jarvis, N.J., 2012. Meta-analysis of the effects of soil properties, site factors and experimental conditions on solute transport. Hydrol. Earth Syst. Sci. 16 (6), 1647–1665. https://doi.org/10.5194/hess-16-1647-2012.

Köhne, J.M., Köhne, S., Šimůnek, J., 2009. A review of model applications for structured soils: a) Water flow and tracer transport. J. Contam. Hydrol. 104 (1–4), 4–35. https://doi.org/10.1016/j.jconhyd.2008.10.002.

Lin, H., Zhou, X., 2008. Evidence of subsurface preferential flow using soil hydrologic monitoring in the Shale Hills catchment. Eur. J. Soil Sci. 59 (1), 34–49. https://doi.org/10.1111/j.1365-2389.2007.00988.x.

Lindahl, A.M.L., Dubus, I.G., Jarvis, N.J., 2009. Site classification to predict the abundance of the deep-burrowing earthworm *Lumbricus terrestris* L. Vadose Zone J. 8 (4), 911–915. https://doi.org/10.2136/vzj2008.140.

Liu, H., Lin, H., 2015. Frequency and control of subsurface preferential flow: from pedon to catchment scales. Soil Sci. Soc. Am. J. 79 (2), 362–377. https://doi.org/10.2136/sssaj2014.08.0330.

Luo, L.F., Lin, H., Halleck, P., 2008. Quantifying soil structure and preferential flow in intact soil using x-ray computed tomography. Soil Sci. Soc. Am. J. 72 (4), 1058–1069. https://doi.org/10.2136/sssaj2007.0179.

Luxmoore, R.J., 1981. Micro-, meso-, and macroporosity of soil. Soil Sci. Soc. Am. J. 45 (3), 671–672. https://doi.org/10.2136/sssaj1981.03615995004500030051x.

McGuire, K.J., Weiler, M., McDonnell, J.J., 2007. Integrating tracer experiments with modeling to assess runoff processes and water transit times. Adv. Water Resour. 30 (4), 824–837. https://doi.org/10.1016/j.advwatres.2006.07.004.

Megahan, W.F., Clayton, J.L., 1983. Tracing subsurface flow on roadcuts on steep, forested slopes. Soil Sci. Soc. Am. J. 47 (6), 1063–1067. https://doi.org/10.2136/sssaj1983.03615995004700060001x.

Mirus, B.B., Nimmo, J.R., 2013. Balancing practicality and hydrologic realism: a parsimonious approach for simulating rapid groundwater recharge via unsaturated-zone preferential flow. Water Resour. Res. 49 (3), 1458–1465. https://doi.org/10.1002/wrcr.20141.

Mosley, M.P., 1982. Subsurface flow velocities through selected forest soils, South Island, New-Zealand. J. Hydrol. 55 (1–4), 65–92. https://doi.org/10.1016/0022-1694(82)90121-4.

Mutema, M., Chaplot, V., Jewitt, G., Chivenge, P., Blöschl, G., 2015. Annual water, sediment, nutrient, and organic carbon fluxes in river basins: a global meta-analysis as a function of scale. Water Resour. Res. 51 (11), 8949–8972. https://doi.org/10.1002/2014wr016668.

Naveed, M., Moldrup, P., Schaap, M.G., Tuller, M., Kulkarni, R., Vogel, H.J., De Jonge, L.W., 2016. Prediction of biopore-and matrix-dominated flow from X-ray CT-derived macropore network characteristics. Hydrol. Earth Syst. Sci. 20 (10), 4017–4030. https://doi.org/10.5194/hess-20-4017-2016.

Negishi, J.N., Noguchi, S., Sidle, R.C., Ziegler, A.D., Nik, A.R., 2007. Stormflow generation involving pipe flow in a zero-order basin of Peninsular Malaysia. Hydrol. Process. 21 (6), 789–806. https://doi.org/10.1002/hyp.6271.

Nimmo, J.R., 2007. Simple predictions of maximum transport rate in unsaturated soil and rock. Water Resour. Res. 43 (5).

Nimmo, J.R., 2012. Preferential flow occurs in unsaturated conditions. Hydrol. Process. 26 (5), 786–789. https://doi.org/10.1002/hyp.8380.

Peng, Z., Tian, F., Hu, H., 2016. Impacts of rainfall features and antecedent soil moisture on occurrence of preferential flow: a study at hillslopes using high-frequency monitoring. Hydrol. Earth Syst. Sci. Discussions 18, 1–22.

Prasad, A.M., Iverson, L.R., Liaw, A., 2006. Newer classification and regression tree techniques: Bagging and random forests for ecological prediction. Ecosystems 9 (2), 181–199. https://doi.org/10.1007/s10021-005-0054-1.

Rawls, W.J., Brakensiek, D.L., Logsdon, S.D., 1993. Predicting saturated hydraulic conductivity utilizing fractal principles. Soil Sci. Soc. Am. J. 57 (5), 1193–1197. https://doi.org/10.2136/sssaj1993.03615995005700050005x.

Rothwell, J.J., Futter, M.N., Dise, N.B., 2008. A classification and regression tree model of controls on dissolved inorganic nitrogen leaching from European forests. Environ. Pollut. 156 (2), 544–552. https://doi.org/10.1016/j.envpol.2008.01.007.

Sidle, R.C., Noguchi, S., Tsuboyama, Y., Laursen, K., 2001. A conceptual model of preferential flow systems in forested hillslopes: evidence of self-organization. Hydrol. Process. 15 (10), 1675–1692. https://doi.org/10.1002/hyp.233.

Sidle, R.C., Tsuboyama, Y., Noguchi, S., Hosoda, I., Fujieda, M., Shimizu, T., 2000. Stormflow generation in steep forested headwaters: a linked hydrogeomorphic paradigm. Hydrol. Process. 14 (3), 369–385. https://doi.org/10.1002/(Sici)1099-1085(20000228)14:3<369::Aid-Hyp943>3.3.Co;2-P.

Šimůnek, J., Jarvis, N.J., van Genuchten, M.T., Gärdenäs, A., 2003. Review and comparison of models for describing non-equilibrium and preferential flow and transport

in the vadose zone. J. Hydrol. 272 (1–4), 14–35. https://doi.org/10.1016/S0022-1694(02)00252-4.
Smettem, K.R.J., Collisgeorge, N., 1985. The influence of cylindrical macropores on steady-state infiltration in a soil under pasture. J. Hydrol. 79 (1–2), 107–114. https://doi.org/10.1016/0022-1694(85)90185-4.
Uchida, T., Kosugi, K., Mizuyama, T., 2001. Effects of pipeflow on hydrological process and its relation to landslide: a review of pipeflow studies in forested headwater catchments. Hydrol. Process. 15 (11), 2151–2174. https://doi.org/10.1002/hyp.281.
Uchida, T., Meerveld, I.T., McDonnell, J.J., 2005. The role of lateral pipe flow in hillslope runoff response: an intercomparison of non-linear hillslope response. J. Hydrol. 311 (1–4), 117–133. https://doi.org/10.1016/j.jhydrol.2005.01.012.
van Schaik, N.L.M.B., Schnabel, S., Jetten, V.G., 2008. The influence of preferential flow on hillslope hydrology in a semi-arid watershed (in the Spanish Dehesas). Hydrol. Process. 22 (18), 3844–3855. https://doi.org/10.1002/hyp.6998.
Weiler, M., 2017. Macropores and preferential flow-a love-hate relationship. Hydrol. Process. 31 (1), 15–19. https://doi.org/10.1002/hyp.11074.
Weiler, M., McDonnell, J.J., 2007. Conceptualizing lateral preferential flow and flow networks and simulating the effects on gauged and ungauged hillslopes. Water Resour. Res. 43 (3).
Weiler, M., Naef, F., 2003. An experimental tracer study of the role of macropores in infiltration in grassland soils. Hydrol. Process. 17 (2), 477–493. https://doi.org/10.1002/hyp.1136.
Wiekenkamp, I., Huisman, J.A., Bogena, H.R., Lin, H.S., Vereecken, H., 2016. Spatial and temporal occurrence of preferential flow in a forested headwater catchment. J. Hydrol. 534, 139–149. https://doi.org/10.1016/j.jhydrol.2015.12.050.
Wienhöfer, J., Germer, K., Lindenmaier, F., Färber, A., Zehe, E., 2009. Applied tracers for the observation of subsurface stormflow at the hillslope scale. Hydrol. Earth Syst. Sci. 13 (7), 1145–1161. https://doi.org/10.5194/hess-13-1145-2009.
Yu, X., Duffy, C., Baldwin, D.C., Lin, H., 2014. The role of macropores and multi-resolution soil survey datasets for distributed surface-subsurface flow modeling. J. Hydrol. 516, 97–106. https://doi.org/10.1016/j.jhydrol.2014.02.055.
Zehe, E., Blume, T., Blöschl, G., 2010. The principle of 'maximum energy dissipation': a novel thermodynamic perspective on rapid water flow in connected soil structures. Phil. Trans. R. Soc. B365 (1545), 1377–1386. https://doi.org/10.1098/rstb.2009.0308.
Zehe, E., Elsenbeer, H., Lindenmaier, F., Schulz, K., Blöschl, G., 2007. Patterns of predictability in hydrological threshold systems. Water Resour. Res. 43 (7), 07434.
Zhu, T.X., 1997. Deep-seated, complex tunnel systems - a hydrological study in a semi-arid catchment, Loess Plateau. China. Geomorphol. 20 (3–4), 255–267. https://doi.org/10.1016/S0169-555x(97)00027-5.
Angermann, L., Jackisch, C., Allroggen, N., Sprenger, M., Zehe, E., Tronicke, J., Weiler, M., Blume, T., 2017. Form and function in hillslope hydrology: characterization of subsurface flow based on response observations. Hydrol. Earth Syst. Sci. 21 (7), 3727–3748. https://doi.org/10.5194/hess-21-3727-2017.
Aubertin, G.M., 1971. Nature and Extent of Macropores in Forest Soils and their Influence on Subsurface Water Movement. USDA Forest Service Report, NE-192.
Beasley, R.S., 1976. Contribution of subsurface flow from upper slopes of forested watersheds to channel flow. Soil Sci. Soc. Am. J. 40 (6), 955–957. https://doi.org/10.2136/sssaj1976.03615995004000060039x.
Buczko, U., Bens, O., Hüttl, R.E., 2006. Tillage effects on hydraulic properties and macroporosity in silty and sandy soils. Soil Sci. Soc. Am. J. 70 (6), 1998–2007. https://doi.org/10.2136/sssaj2006.0046.
Buttle, J.M., McDonald, D.J., 2002. Coupled vertical and lateral preferential flow on a forested slope. Water Resour. Res. 38 (5) 106010.1029/2001wr000773.
Casey, F.X.M., Logsdon, S.D., Horton, R., Jaynes, D.B., 1998. Measurement of field soil hydraulic and solute transport parameters. Soil Sci. Soc. Am. J. 62 (5), 1172–1178. https://doi.org/10.2136/sssaj1998.03615995006200050003x.
Clothier, B.E., Smettem, K.R.J., 1990. Combining laboratory and field measurements to define the hydraulic properties of Soil. Soil Sci. Soc. Am. J. 54 (2), 299–304. https://doi.org/10.2136/sssaj1990.03615995005400020001x.
Cullum, R.F., 2009. Macropore flow estimations under no-till and till systems. Catena 78 (1), 87–91. https://doi.org/10.1016/j.catena.2009.03.004.
Edwards, W., Van der Ploeg, R., Ehlers, W., 1979. A numerical study of the effects of noncapillary-sized pores upon infiltration. Soil Sci. Soc. Am. J. 43 (5), 851–856. https://doi.org/10.2136/sssaj1979.03615995004300050007x.
Everts, C.J., Kanwar, R.S., 1990. Estimating preferential flow to a subsurface drain with tracers. Trans. ASAE 33 (2), 451–457. https://doi.org/10.13031/2013.31350.
Feyen, H., Wunderli, H., Wydler, H., Papritz, A., 1999. A tracer experiment to study flow paths of water in a forest soil. J. Hydrol. 225 (3–4), 155–167. https://doi.org/10.1016/S0022-1694(99)00159-6.
Frey, S.K., Rudolph, D.L., 2011. Multiscale characterization of vadose zone macroporosity in relation to hydraulic conductivity and subsurface drainage. Soil Sci. Soc. Am. J. 75 (4), 1253–1264. https://doi.org/10.2136/sssaj2010.0403.
Frey, S.K., Rudolph, D.L., Conant, B., 2012. Bromide and chloride tracer movement in macroporous tile-drained agricultural soil during an annual climatic cycle. J. Hydrol. 460, 77–89. https://doi.org/10.1016/j.jhydrol.2012.06.041.
Germann, P., Beven, K., 1981. Water flow in soil macropores.1. An experimental approach. J Soil Sci. 32 (1), 1–13. https://doi.org/10.1111/j.1365-2389.1981.tb01681.x.
Graham, C.B., Woods, R.A., McDonnell, J.J., 2010. Hillslope threshold response to rainfall: (1) A field based forensic approach. J. Hydrol. 393 (1–2), 65–76. https://doi.org/10.1016/j.jhydrol.2009.12.015.
Hallard, M., Armstrong, A.C., 1992. Observations of water movement to and within mole drainage channels. J. Agr. Eng. Res. 52 (4), 309–315. https://doi.org/10.1016/0021-8634(92)80069-5.
Jackson, C.R., Du, E., Klaus, J., Griffiths, N.A., Bitew, M., McDonnell, J.J., 2016. Interactions among hydraulic conductivity distributions, subsurface topography, and transport thresholds revealed by a multitracer hillslope irrigation experiment. Water Resour. Res. 52 (8), 6186–6206. https://doi.org/10.1002/2015wr018364.
Jacobsen, O.H., Moldrup, P., Larsen, C., Konnerup, L., Petersen, L.W., 1997. Particle transport in macropores of undisturbed soil columns. J. Hydrol. 196 (1–4), 185–203. https://doi.org/10.1016/S0022-1694(96)03291-X.
Jaynes, D.B., Ahmed, S.I., Kung, K.J.S., Kanwar, R.S., 2001. Temporal dynamics of preferential flow to a subsurface drain. Soil Sci. Soc. Am. J. 65 (5), 1368–1376. https://doi.org/10.2136/sssaj2001.6551368x.
Joerin, C., Beven, K.J., Musy, A., Talamba, D., 2005. Study of hydrological processes by the combination of environmental tracing and hill slope measurements: application on the Haute-Mentue catchment. Hydrol. Process. 19 (16), 3127–3145. https://doi.org/10.1002/hyp.5836.
Kienzler, P.M., Naef, F., 2008. Subsurface storm flow formation at different hillslopes and implications for the 'old water paradox'. Hydrol. Process. 22 (1), 104–116. https://doi.org/10.1002/hyp.6687.
Kim, H., Anderson, S.H., Motavalli, P.P., Gantzer, C.J., 2010. Compaction effects on soil macropore geometry and related parameters for an arable field. Geoderma 160 (2), 244–251. https://doi.org/10.1016/j.geoderma.2010.09.030.
Kim, Y.J., Darnault, C.J.G., Bailey, N.O., Parlange, J.Y., Steenhuis, T.S., 2005. Equation for describing solute transport in field soils with preferential flow paths. Soil Sci. Soc. Am. J. 69 (2), 291–300. https://doi.org/10.2136/sssaj2005.0291.
Kitahara, H., 1993. Characteristics of pipe flow in forested slopes. IAHS Publ. 212, 235–242.
Klaus, J., Zehe, E., Elsner, M., Palm, J., Schneider, D., Schröder, B., Steinbeiss, S., van Schaik, L., West, S., 2014. Controls of event-based pesticide leaching in natural soils: A systematic study based on replicated field scale irrigation experiments. J. Hydrol. 512, 528–539. https://doi.org/10.1016/j.jhydrol.2014.03.020.
Kung, K.J.S., Kladivko, E.J., Gish, T.J., Steenhuis, T.S., Bubenzer, G., Helling, C.S., 2000a. Quantifying preferential flow by breakthrough of sequentially applied tracers: silt loam soil. Soil Sci. Soc. Am. J. 64 (4), 1296–1304. https://doi.org/10.2136/sssaj2000.6441296x.
Kung, K.J.S., Steenhuis, T.S., Kladivko, E.J., Gish, T.J., Bubenzer, G., Helling, C.S., 2000b. Impact of preferential flow on the transport of adsorbing and non-adsorbing tracers. Soil Sci. Soc. Am. J. 64 (4), 1290–1296. https://doi.org/10.2136/sssaj2000.6441290x.
Laine-Kaulio, H., Backnäs, S., Karvonen, T., Koivusalo, H., McDonnell, J.J., 2014. Lateral subsurface stormflow and solute transport in a forested hillslope: a combined measurement and modeling approach. Water Resour. Res. 50 (10), 8159–8178. https://doi.org/10.1002/2014wr015381.
Lange, J., Kopp, B.J., Bents, M., Menzel, L., 2015. Tracing variability of run-off generation in mountainous permafrost of semi-arid north-eastern Mongolia. Hydrol. Process 29 (6), 1046–1055. https://doi.org/10.1002/hyp.10218.
Laubel, A., Jacobsen, O.H., Kronvang, B., Grant, R., Andersen, H.E., 1999. Subsurface drainage loss of particles and phosphorus from field plot experiments and a tile-drained catchment. J. Environ. Qual. 28 (2), 576–584. https://doi.org/10.2134/jeq1999.00472425002800020023x.
Li, X.Y., Hu, X., Zhang, Z.H., Peng, H.Y., Zhang, S.Y., Li, G.Y., Li, L., Ma, Y.J., 2013. Shrub hydropedology: preferential water availability to deep soil layer. Vadose Zone J. 12 (4). https://doi.org/10.2136/vzj2013.01.0006.
Luo, L.F., Lin, H., Schmidt, J., 2010. Quantitative relationships between soil macropore characteristics and preferential flow and transport. Soil Sci. Soc. Am. J. 74 (6), 1929–1937. https://doi.org/10.2136/sssaj2010.0062.
McCaig, M., 1983. Contributions to storm quickflow in a small headwater catchment – the role of natural pipes and soil macropores. Earth Surf. Processes Landforms 8 (3), 239–252. https://doi.org/10.1002/esp.3290080306.
McDaniel, P.A., Regan, M.P., Brooks, E., Boll, J., Barndt, S., Falen, A., Young, S.K., Hammel, J.E., 2008. Linking fragipans, perched water tables, and catchment-scale hydrological processes. Catena 73 (2), 166–173. https://doi.org/10.1016/j.catena.2007.05.011.
Mehlhorn, J., Armbruster, F., Uhlenbrook, S., Leibundgut, C., 1998. Determination of the geomorphological instantaneous unit hydrograph using tracer experiments in a headwater basin. IAHS Publ. 248, 327–335.
Messing, I., Jarvis, N.J., 1993. Temporal variation in the hydraulic conductivity of a tilled clay soil as measured by tension infiltrometers. J. Soil Sci. 44 (1), 11–24. https://doi.org/10.1111/j.1365-2389.1993.tb00430.x.
Mikovari, A., Peter, C., Leibundgut, C., 1995. Investigation of preferential flow using tracer techniques. IAHS Publ. 229, 87–97.
Mohanty, B.P., Bowman, R.S., Hendrickx, J.M.H., van Genuchten, M.T., 1997. New piecewise-continuous hydraulic functions for modeling preferential flow in an intermittent-flood-irrigated field. Water Resour. Res. 33 (9), 2049–2063. https://doi.org/10.1029/97wr01701.
Mosley, M.P., 1979. Streamflow generation in a forested watershed. N. Z. Water Resour. Res. 15 (4), 795–806. https://doi.org/10.1029/WR015i004p00795.
Noguchi, S., Tsuboyama, Y., Sidle, R.C., Hosoda, I., 1999. Morphological characteristics of macropores and the distribution of preferential flow pathways in a forested slope segment. Soil Sci. Soc. Am. J. 63 (5), 1413–1423. https://doi.org/10.2136/sssaj1999.6351413x.
Nyberg, L., Rodhe, A., Bishop, K., 1999. Water transit times and flow paths from two line injections of 3H and 36Cl in a microcatchment at Gardsjon, Sweden. Hydrol. Process 13 (11), 1557–1575. https://doi.org/10.1002/(Sici)1099-1085(19990815)13:11<1557::Aid-Hyp835>3.0.Co;2-S.
Paradelo, M., Katuwal, S., Moldrup, P., Norgaard, T., Herath, L., de Jonge, L.W., 2016. X-ray CT-derived soil characteristics explain varying air, water, and solute transport properties across a loamy field. Vadose Zone J. 15 (4). https://doi.org/10.2136/vzj2015.07.0104.

Pilgrim, D.H., Huff, D.D., Steele, T.D., 1978. Field evaluation of subsurface and surface runoff.2. runoff processes. J. Hydrol. 38 (3–4), 319–341. https://doi.org/10.1016/0022-1694(78)90077-X.

Rachman, A., Anderson, S.H., Gantzer, C.J., Alberts, E.E., 2004. Soil hydraulic properties influenced by stiff-stemmed grass hedge systems. Soil Sci. Soc. Am. J. 68 (4), 1386–1393. https://doi.org/10.2136/sssaj2004.1386.

Retter, M., Kienzler, P., Germann, P.F., 2006. Vectors of subsurface stormflow in a layered hillslope during runoff initiation. Hydrol. Earth Syst. Sci. 10 (3), 309–320. https://doi.org/10.5194/hess-10-309-2006.

Richards, T.L., Steenhuis, T.S., 1988. Tile drain sampling of preferential flow on a field scale. J. Contam. Hydrol. 3, 307–325. https://doi.org/10.1016/0169-7722(88)90038-1.

Scaini, A., Audebert, M., Hissler, C., Fenicia, F., Gourdol, L., Pfister, L., Beven, K.J., 2017. Velocity and celerity dynamics at plot scale inferred from artificial tracing experiments and time-lapse ERT. J. Hydrol. 546, 28–43. https://doi.org/10.1016/j.jhydrol.2016.12.035.

Schneider, P., Pool, S., Strouhal, L., Seibert, J., 2014. True colors – experimental identification of hydrological processes at a hillslope prone to slide. Hydrol. Earth Syst. Sci. 18 (2), 875–892. https://doi.org/10.5194/hess-18-875-2014.

Seyfried, M.S., Rao, P.S.C., 1987. Solute transport in undisturbed columns of an aggregated tropical soil – preferential flow effects. Soil Sci. Soc. Am. J. 51 (6), 1434–1444. https://doi.org/10.2136/sssaj1987.03615995005100060008x.

Shaw, J.N., West, L.T., Radcliffe, D.E., Bosch, D.D., 2000. Preferential flow and pedotransfer functions for transport properties in sandy Kandiudults. Soil Sci. Soc. Am. J. 64 (2), 670–678. https://doi.org/10.2136/sssaj2000.642670x.

Smettem, K.R.J., Kirkby, C., 1990. Measuring the hydraulic properties of a stable aggregated soil. J. Hydrol. 117 (1–4), 1–13. https://doi.org/10.1016/0022-1694(90)90084-B.

Tanaka, T., Yasuhara, M., Sakai, H., Marui, A., 1988. The Hachioji experimental basin study – storm runoff processes and the mechanism of its generation. J. Hydrol. 102 (1–4), 139–164. https://doi.org/10.1016/0022-1694(88)90095-9.

Tromp-van Meerveld, H.J., McDonnell, J.J., 2006. Threshold relations in subsurface stormflow: 2. the fill and spill hypothesis. Water Resour. Res. 42 (2) DOI:W0241110.1029/2004wr003800.

Tsuboyama, Y., Sidle, R.C., Noguchi, S., Hosoda, I., 1994. Flow and solute transport through the soil matrix and macropores of a hillslope segment. Water Resour. Res. 30 (4), 879–890. https://doi.org/10.1029/93wr03245.

Uchida, T., Kosugi, K., Mizuyama, T., 1999. Runoff characteristics of pipeflow and effects of pipeflow on rainfall-runoff phenomena in a mountainous watershed. J. Hydrol. 222 (1–4), 18–36. https://doi.org/10.1016/S0022-1694(99)00090-6.

Udawatta, R.P., Anderson, S.H., 2008. CT-measured pore characteristics of surface and subsurface soils influenced by agroforestry and grass buffers. Geoderma 145 (3–4), 381–389. https://doi.org/10.1016/j.geoderma.2008.04.004.

Villholth, K.G., Jensen, K.H., Fredericia, J., 1998. Flow and transport processes in a macroporous subsurface-drained glacial till soil – I: field investigations. J. Hydrol. 207 (1–2), 98–120. https://doi.org/10.1016/S0022-1694(98)00129-2.

Weiler, M., Naef, F., Leibundgut, C., 1998. Study of runoff generation on hillslopes using tracer experiments and a physically-based numerical hillslope model. IAHS Publ. 248, 353–360.

Zehe, E., Flühler, H., 2001. Preferential transport of isoproturon at a plot scale and a field scale tile-drained site. J. Hydrol. 247 (1–2), 100–115. https://doi.org/10.1016/S0022-1694(01)00370-5.

Zhang, Z.B., Zhou, H., Zhao, Q.G., Lin, H., Peng, X., 2014. Characteristics of cracks in two paddy soils and their impacts on preferential flow. Geoderma 228, 114–121. https://doi.org/10.1016/j.geoderma.2013.07.026.